

LIU Jing

Cooling strategies and transport theories for brain hypothermia resuscitation

© Higher Education Press and Springer-Verlag 2007

Abstract The brain is one of the most important organs in a biological body whose normal function depends heavily on an uninterrupted delivery of oxygen. Unlike skeletal muscles that can survive for hours without oxygen, neuron cells in the brain are easily subjected to an irreversible damage within minutes from the onset of oxygen deficiency. With the interruption of cardiopulmonary circulation in many cardiac surgical procedures or accidental events leading to cerebral circulation arrest, an imbalance between energy production and consumption will occur which causes a rapid depletion of oxygen due to the interrupted blood-flow to the brain. Meanwhile, the cooling function of the blood flow on the hot tissue will be stopped, while metabolic heat generation in the tissues still keeps running for awhile. Under such adverse situations, the potential for cerebral protection through hypothermia has been intensively investigated in clinics by lowering brain temperature to restrain the cerebral oxygen demands. The reason can be attributed to the decreased metabolic requirements of the cold brain tissues, which allows a longer duration for the brain to endure reduced oxygen delivery. It is now clear that hypothermia would serve as the principal way for neurologic protection in a wide variety of emergency medicines, especially in cerebral damage, anoxia, circulatory arrest, respiratory occlusion, etc. However, although brain cooling has been found uniquely significant in clinical practices, the serious lack of knowledge on the mechanisms involved prevents its further advancement in brain resuscitation. Compared with the expanded trials in clinics, only very limited efforts were made to probe the engineering issues involved, which turns out to be a major obstacle for the successful operation of brain hypothermia resuscitation. From the viewpoint of biothermal medical engineering, the major theories and strategies for

administering brain cooling can generally be classified into three categories: heat transfer, oxygen transport and cooling strategy. Aiming to provide a complete overview of the brain hypothermia resuscitation, this article comprehensively summarizes the recent progresses made in theoretical, practical and experimental techniques in the area. Particularly, attention is paid to the mathematical models to quantify the heat and oxygen transport inside the cerebral tissues. Typical cooling strategies to effectively lower brain temperature and thus decrease oxygen consumption rate in the cerebral tissues are analyzed. Approaches to deliver oxygen directly to the target tissues are discussed. Meanwhile, some future efforts worth pursuing within the area of brain cooling are suggested.

Keywords brain cooling, oxygen transport, bioheat transfer, tissue vasculature, circulation arrest, compartmental model, cerebral hemodynamics, brain hypothermia resuscitation, volumetric cooling, cerebral hypoxia

1 Introduction

As one of the most important organs in a biological body, the brain's normal function depends heavily on an uninterrupted delivery of oxygen, whose level and consumption dynamics often determine the physiological behaviors of biological bodies either at the tissue or cellular level. Sufficient supply of oxygen allows the nerve cells, consisting of the information processing unit of the brain, to appropriately function or even survive. Unlike skeletal muscles that can survive for hours without oxygen, brain neuron cells are easily subjected to an irreversible damage within minutes from the onset of oxygen deficiency such as in the situation of anoxia [1]. A possible mechanism for such result can be attributed to the distinctive dendritic structure of the nerve cell [2], which serves to enhance oxygen transport and in turn, oxygen depletion.

As is well known, oxygen transport relies on the blood flow in living tissues. In a normal state, the cerebral circulation is under control by many regulatory mechanisms acting

Received August 25, 2006; accepted November 17, 2006

LIU Jing (✉)

Technical Institute of Physics and Chemistry, Chinese Academy of Sciences, Beijing 100080, China

Department of Biomedical Engineering, School of Medicine, Tsinghua University, Beijing 100084, China

E-mail: jliu@cl.cryo.ac.cn

on the vascular bed to maintain an appropriate cerebral blood flow and adequate oxygen. However, in a pathological state, the hemodynamic parameters, such as blood flow, vascular resistance and diameters, etc., will significantly change compared with their normal ranges [3–6]. Especially when cerebral circulation arrest occurs, such as in the interruption of cardiopulmonary circulation in many cardiac surgical procedures or accidental events [7,8], the cerebral perfusion pressure will decrease from its normal level and the cerebral blood flow related to this pressure is also lowered. Then an imbalance between energy production and consumption will occur, which subsequently causes a rapid loss of oxygen and depletion of the metabolic substrate because the decreasing blood flow is no longer able to supply sufficient oxygen or nutrient to the tissues [9–12]. In clinics, the current survival rate from out-of-hospital cardiac arrest is poor, since cells in the brain and heart begin to die within minutes. Similar difficulties also pertain to stroke patients. Except for the pathological state, the blood flow in fact plays a rather important role in a variety of daily life situations. For example, the brain usually consumes high amounts of oxygen and other nutrients and is accompanied by an intense heat production. However, its temperature is generally kept at a stable, tightly regulated homeostatic state. This is mainly attributed to cerebral circulation, which plays a crucial role in dissipating this potentially dangerous metabolic heat from brain tissue [11]. It has been suggested that in passive and exercise hyperthermia the brain may be protected against thermal damage by a mechanism of selective brain cooling (SBC), which brings about suppression of the temperature of the brain, rendering it significantly lower than the trunk and arterial blood temperature [12]. In the extreme instances when brain hyperthermia becomes serious, both exposure to heat and intense physical activity in a hot, humid environment restrict heat dissipation from the brain and may push its temperatures to the limits of physiological functions [11]. Brain hyperthermia may also result from metabolic activation induced by various addictive drugs [11], such as heroin, cocaine, and meth-amphetamine, whose thermogenic effects can even be enhanced during physiological activation. Therefore, uncontrollable use of amphetamine-like drugs under conditions restricting heat dissipation from the brain may result both in acute life threatening complications and clinically latent but dangerous morphological and functional brain destruction [11].

Up to now, it has been accepted that cerebral hypothermia is by far the most principal means of neurologic protection during cardiac operations, especially for procedures requiring reduced perfusion or circulatory arrest [13]. When circulatory arrest occurs, hypothermia is commonly applied to prevent overheating, which is a result of decreased cooling by lowered cerebral blood flow, continuous oxygen consumption and metabolic heat generation [1,7,8]. The efficacy of hypothermia in preserving neurological function when instituted before and during certain no-flow cardiovascular states has in fact been documented both clinically and experimentally in animals since the 1950s [14–16]. Many

believe that the ability of cells to survive ischemia could be significantly enhanced by rapid cooling of the heart and brain, i.e., by resuscitative hypothermia [17]. Lowering the brain temperature would aid in decreasing the cerebral oxygen and metabolic demands. Reported experiments suggested that the brain continues to metabolize at a very low base rate during deep hypothermic circulatory arrest [18]. Therefore, efficient cooling allows a long duration for the brain to have reduced oxygen delivery, although other mechanisms may also contribute to it.

There have been many discussions on the effect of hypothermia and circulatory arrest on cerebral blood flow and metabolism [1,7,8]. Some studies have found that total circulatory arrest allows patients to survive for 60 min or more at 15–18°C without any subsequent cerebral dysfunction, and hypothermia is effective for protection against both global and focal brain ischemia. In laboratory studies, mild hypothermia (34°C) was discovered to mitigate brain damage significantly after cardiac arrest [19]. Therefore, mild or moderate hypothermia (>30°C) has been proposed for clinical use as a therapeutic option for achieving protection from cerebral ischemia in brain injury patients [20]. Clinical tests demonstrate that, the best hope for a long-term survival after cardiac arrest could begin by inducing mild hypothermia to minimize neurologic damage [21]. Such strategy also has possible application in patients with stroke, spinal cord and traumatic brain injury, septic shock, and myocardial infarction [21]. The low temperature is usually achieved by systemic body cooling, or almost entirely by ventilating cold blood during hypothermic cardiopulmonary bypass, whose mechanism is convection [22,23]. Nevertheless, timely and safe delivery of hypothermia remains a big clinical challenge. To maximize neuroprotection yet minimize systemic complications, ultra-early delivery of selective cerebral hypothermia would be advantageous [13].

Up to now, knowledge on the thermal behaviors of the human brain either in normal or pathological state is still very limited. Overall, previous major engineering efforts towards realizing a highly efficient brain cooling can be classified into three categories such as cooling strategy, heat transfer and oxygen transport. Following this category, some of the most typical issues will be discussed in this paper.

2 Cooling strategies for brain hypothermia resuscitation

2.1 Significance of SBC

As mentioned above, the brain usually works in a stable state, although very sensitive to heat stress [24]. This is mainly attributed to the mechanism of SBC, which guarantees a local hypothermic neuroprotection while minimizing the deleterious side-effects of systemic hypothermia. It is thus necessary for animals or human beings to maintain a normal physiological status. SBC is defined as a brain temperature that is

cooler than the temperature of the arterial blood from the trunk. It will be enhanced during heat exposure, endurance exercise, relaxed wakefulness, and vanish in the cold and during emotional distress. Overall, SBC is a multifunctional effector mechanism, integrating both thermal and non-thermal regulatory functions [25]. It is generally considered that its role is to: protect the brain from heat damage; intensify in dehydrated mammals, thereby saving water; help exercising animals to delay exhaustion; thermally modulate alertness; help diving animals to have their cerebral temperature drop much lower than normal levels, expanding diving capacity and protecting the brain from asphyxic damage [25].

The mechanism of SBC allows the brain to remain cooler than the rest of the body. In mammals, SBC during hyperthermia has been demonstrated to work well. It is achieved in some species (e.g., cats, dogs, sheep) by thermally conditioning the carotid blood prior to its entering the circle of Willis [26–29]. A countercurrent heat exchange occurs in the network of fine vessels (the carotid *rete*) in contact with cranial venous plexuses and lakes receiving cool venous blood from the systemic heat exchanger of the head (skin, nasal mucosa, ear pinna, horn). To test the critical level of body temperature beyond which animals will not continue to exercise voluntarily in the heat, Fuller et al. measured brain and abdominal temperatures in eight male Sprague-Dawley rats (350–450 g) exercising voluntarily to a point of fatigue in two hot environments [30]. It was found that, brain temperature was higher than abdominal temperature throughout the exercise. SBC did not occur when body temperature was below the level limiting exercise. Artiodactyls employ SBC regularly during experimental hyperthermia. In free-ranging antelopes, however, SBC was often present when body temperature was low but absent when brain temperature was near 42°C. Some researchers think that [31], the primary effect of SBC is to adjust the activity of the heat loss mechanisms to the magnitude of the heat stress rather than to protect the brain from thermal damage.

When SBC was extended to humans, researchers proposed some controversial notions [32,33]. There generally includes two heat-exchangers for the SBC to limit the increase of intracranial heat [24]. The first one, in the face and scalp, disperses calories through sweat evaporation. The second one is intracranial, close to the arteries which irrigate the brain. They are connected by a vascular network. In these situations, the arterial blood temperature, upon which cerebral temperature depends upon, is reduced by the cooled venous blood coming from subcutaneous tissues through the skull wall [24]. Among existing theoretical analysis conducted to estimate the effect of countercurrent heat exchange and heat conduction on the extent of SBC in the artery, Nielsen [34] estimated that the cooling strength is only 0.02°C per centigrade difference between arterial and venous temperatures. In another analysis given by Zhu [35], contribution from heat conduction was found to be comparable to the countercurrent heat exchange and can account for more than 41% of the total

heat loss provided that the neck skin temperature is low in SBC. Study on a sheep showed that SBC depended mainly on the heat loss from the nasal mucosa [36]. Some experiments also supported the idea that the brain can be cooled, at its outer front aspects, by heat loss from the upper respiratory tract [37]. The question of whether SBC has influence on human brain temperature is not likely to be resolved without direct measurement of intracranial temperature [38,39]. Due to practical difficulty in measurement, the efficacy of SBC in humans, in which cooled venous blood from the heat exchange of the head lowers the temperature of the arterial blood, in turn, cools the brain, is unclear. However, it is certain that SBC does occur in hyperthermic humans despite the fact that humans have no carotid *rete*, a vascular structure that facilitates countercurrent heat exchange located at the base of the skull in some mammals [40]. Up to now, there exist overwhelming evidences in favor of human SBC. SBC has in fact been well-accepted now either in animals or humans [32]. The major components of the SBC system in humans are generally emissary and angular veins, upper respiratory tract, tympanic cavity and cerebrospinal fluid. The efficiency of SBC is increased by evaporation of sweat on the head and by ventilation through the nose [40]. Given the near-normal initial rectal temperature, preferential brain cooling may have been at least partially responsible for the positive neurologic outcome [41].

Except for the above cases, selectively lowering temperature of the specific organs or tissues is also critical in a series of important clinical situations. For example, during hyperthermia in the human body caused by high environmental temperature, increased neural activities, fever, or whole-body thermal therapy, the body core temperature can rise to as high as 42°C [32]. This high trunk temperature may endanger the brain tissues, which are extremely heat-susceptible and do not tolerate high temperature. It is therefore necessary to introduce a rapid localized-cooling as an emergency care approach to alleviate brain overheating (especially at the deep part of the brain), except for the heat dissipation from the outer surface of the head, face, and upper respiratory tract and the specialized vasculature keeping the brain cool. Besides, the localized cooling is also critical to prevent the healthy tissues from burning injury during a deep brain tumor hyperthermia.

There generally exist two distinct types of SBCs [25]: (1) using precooling of arterial blood destined for the brain to cool it, with cool venous blood returning from the nose and head skin; (2) using venous blood to cool the brain directly. Clinically, although the whole body hypothermia can be applied as an alternative to SBC to treat the injured brain (e.g., after hypoxic events) [42], it may induce stronger side effects such as hemodynamic instability, coagulopathy and infection. Therefore, cooling the brain selectively without changing the core temperature is rather important in clinics. That is in fact one of the major reasons why intentionally administrated SBC received tremendous attention among

current investigations. Another disadvantage inherited in a systemic body cooling is its substantial slow cooling rate because the conductive heat loss through the skull surface or countercurrent heat exchange is minimal [7,23,32,43,44]. In general, such hypothermia will have to be performed for several hours or even longer to achieve the desired temperature. Using newborn swine as the test animal, Laptook et al. measured and compared the brain temperature and cerebral blood flow (CBF) during head and body cooling, with and without systemic hypoxemia [45]. It was found that, brain hypothermia achieved through the head or body cooling results in different brain temperature gradients and reductions of global CBF and O₂ uptake. That means the mode of brain cooling will affect the efficacy of modest hypothermia as a neuroprotective therapy. To investigate the effect of selective hypothermia of the brain on regional cerebral blood flow and tissue metabolism, Ibayashi et al. [46] developed a water-cooled metallic plate thermo-regulator placed on the surface of the rats' scalp, from which brain temperature can be precisely modulated with ease. It was found that: (1) the thermo-regulator is useful in small animal experiments; (2) regional brain temperature regulates regional cerebral blood flow; and (3) SBC, even started after forebrain ischemia, ameliorates the derangement of brain metabolism. This suggests the effectiveness of SBC as a cytoprotective strategy.

2.2 Surface cooling

Till now, there is still no ideal way for the efficient cooling of the brain. In general practice, hypothermia is still mainly induced by placing the patients on a mattress with a cover that delivers cold air or liquid over the body. Clinicians also removed patients' clothing and apply cold packs to their heads and torsos. Application of cold forced air to the cranial surface resulted in brain temperatures that were cooler than those observed during hypothermic cardiopulmonary bypass (CPB) without pericranial cooling. On the basis of the assumption that similar beneficial brain temperature changes can be induced in humans, researchers speculate that selective convective brain cooling may enable clinicians to improve neurologic outcome after hypothermic CPB [47]. Improving the efficiency of air hypotherms by increasing the velocity of the cooling current and using a special device for cooling the head coverings has made possible the creation of apparatuses for cranio-cerebral hypothermia in which air is used in the capacity of coolant. This can partially fulfill the requirement of treating patients with open skull-brain injuries and during the post-operative period of neurosurgery [48].

Except for cooling the brain by flow, other surface cooling methods were also tried in the past. For example, a thermoelectric device was used for cooling the brain in cases of head injury [49]. Clinical tests showed that the surface of the brain of a patient could be cooled to 1°C within 40–50 min, and in the deep structures of the brain the temperature dropped to 22°C. However, according to many later researches, such

result is unlikely to occur. Anyway, a high refrigerating capacity of an electronic refrigerator still possibly permits a beneficial regulation of the thermal regime of the entire patient. Some commercially available brain cooling apparatus was just made in this way. Using a head-cooling cap perfused with cold water (5–24 °C), Tooley et al. examined whether the brain could be cooled to below the rectal temperature in a piglet hypoxia ischemia model for a period of 24 h [50]. It was demonstrated that the head-cooling cap can possibly decrease the brain temperature more than that of the body for a 24-hour period while keeping the core temperature mildly hypothermic. Caps were also designed to cool the brains of babies born with oxygen deprivation during birth to prevent brain damage [51]. While the cap offered a moderate overall reduction in brain damage, by about 10 percent, the most promising results were among babies who suffered moderate damage at birth. Those affected by motor damage, such as cerebral palsy, had brain damage reductions of almost 60 percent. Wang et al. [13] developed a cooling helmet, which can deliver initial rapid SBC and maintain a significant temperature gradient between the core and brain temperatures throughout the hypothermic period to provide sufficient regional hypothermia yet minimize systemic complications. Among the experiments on brain cooling during circulatory arrest, Olsen et al. demonstrated that isolated head cooling, whether with frozen liquid or a cooling helmet, is not very effective in actual situations [43].

Overall, nearly all of the previous experiments suggested that surface cooling had a rather limited effect on lowering the brain temperature. Therefore, alternative cooling other than this should be developed for a rapid brain cooling required for cerebral protection during hypothermia resuscitation.

2.3 Cooling through natural cavity

During surface cooling, the brain temperature is reduced while the core temperature remains almost unchanged. Therefore, researchers turn to other ways for brain cooling. Nasopharyngeal cooling was found to enable rapid and selective reductions in cortical and subcortical temperatures without disturbing the recovery of systemic circulation after resuscitation [52]. Trubel et al. performed an animal experiment to investigate the changes in brain temperature through cooling from the pharynx [53]. Significant cooling of the cortex was found in a rodent model. This approach may offer distinct advantages over other methods such as whole-body cooling and externally implemented SBC. Mariak et al. presented a report on human intracranial temperature in conscious patients during and after an upper respiratory bypass [54]. The results support the view that cooling of the upper airway can directly influence human brain temperature. Harris et al. [55] showed that concurrent gas ventilation may mitigate heat-diffusion limitations in liquid breathing, perhaps via bubble-induced turbulence.

In nature, local cooling of the brain by respiration has been found in many animal species with a rete mirabile in the carotid artery/cavernous sinus complex [56]. The mechanism is based on cooling of the nasal vein blood and heat transfer in the cavernous sinus/carotid artery complex and is therefore not active in anaesthetised, intubated animals [57]. Some experiments show that it may be possible to protect the brain in intubated animals and humans from heat-induced damages by establishment of nasal flushing. Even an animal species without a rete mirabile is able to decrease the brain temperature through nasal cooling, which is probably connected to the blood flow. If the results can be extrapolated to humans (no rete mirabile), brain temperature can be decreased by nasal flushing with air or oxygen in intubated patients with hyperthermia. It was suggested that this simple treatment will reduce the infarct volume after head injury, trauma, or brain ischemia [56]. Researchers also performed tests on seven healthy young men participating in six trials with three different types of local cooling [cool air breathing (CAB), face skin cooling, and combined cooling] in a warm environment for 90 min while either resting or exercising on a cycle ergometer with an external work load of 90 W [58]. The results suggest that head skin cooling causes a reduction in heat strain, while CAB does not. This beneficial influence does not, however, appear to be the result of selective brain cooling.

2.4 Cooling through perfusing cold blood

Considering the fact that most of the currently existing cooling methods were slow, could induce only brain surface cooling, or result in systemic reaction, an alternative temperature-lowering strategy, such as cooling through perfusing cold blood was then suggested [21]. Some tests indicated that femoral-carotid hypothermic bypass would rapidly induce a state of SBC without causing systemic hypothermia or hemodynamic instability [59].

Physiologically, regional head and brain cooling was affected in dogs via an extracorporeal blood cooling circuit. Luan et al. shows that cerebral local cooling infusion could reduce stroke-mediated brain injury by inhibiting inflammatory responses [60]. The brain hypothermia induced by local pre-reperfusion infusion ameliorated brain inflammation from stroke. Hansebout et al. compared various physical methods employed for attempted maintenance of homeostatic heart temperatures [61]. Sumbatov et al. proposed to cool the brain by shunting the blood from the femoral artery into the carotid artery, i.e., autoperfusion, and equivalent heating by inserting a special probe-heat exchanger through the femoral vein into the inferior vena cava [62]. As the experiment showed, on coordinating the regimes of cooling the head and equivalent heating of the trunk and limbs, it was possible to restrict hypothermy just to the head region. Such simultaneous oppositely directed dual thermal effect on an organism satisfactorily solves the problem of strict local hypothermy of the brain for safe disconnection of cerebral circulation for a sufficiently long time for neurosurgical purposes.

Despite the potential benefits, few studies have addressed heat transfer difficulties associated with attempting resuscitative hypothermia without bypass procedures. Some researchers proposed to use slurry as an efficient coolant for brain cooling, due to the fact that ice particle slurries can have up to 10 times the cooling capacity of single-phase coolants such as chilled saline [17]. The carotid artery, jugular vein, and lungs are used as in-body ice slurry heat exchangers to achieve rapid targeted cooling of the heart and brain. Slurries are compatible with human tissue and have the needed fluidity to be administered through small-diameter tubing and hypodermic needles. Experiment on swine produced heart and brain cooling rates 20 times greater than conventional methods. In another study [63], Li et al. demonstrated that local brain cooling, produced by local infusion of cold saline prior to reperfusion, could induce long-term functional improvement after stroke. No significant difference in motor performance was observed between the brain cooling infusion and normal control groups. Ding et al. demonstrated that local infusion of saline into ischemic territory could induce regional brain cooling and neuroprotection [64]. Clinically, this procedure could be used in acute stroke treatment, possibly in combination with intra-arterial thrombolysis or mechanical disruption of clot by means of a microcatheter. Further, it was successfully shown that direct retrograde hypothermic perfusion via the jugular vein without cardiopulmonary bypass protected the rat brain after heat stroke. This technique cooled the brain but did not significantly interfere with body temperature [65]. Furuse et al. evaluated cerebral metabolic change during brain hypothermia with intravascular perfusion of cooled crystalloid solution using an extracorporeal cooling-filtration system and cerebroprotective effects of this hypothermia on brain injury in an animal model [66]. The result suggested that brain hypothermia via intra-arterial cooling with an extracorporeal cooling-filtration system had potential to achieve successful, safe, selective brain cooling. Kuhnén et al. presented a technique for isolated brain cooling in pigs by cooling the natural blood supply of the brain [67]. Under general anesthesia both common carotid arteries were exteriorized. One proximal carotid artery was connected to both distal carotid arteries and a heat exchanger in this line to control brain temperature. The second proximal carotid artery was connected to an external jugular vein and a heat exchanger in this arteriovenous shunt was used to clamp trunk temperature. Re-establishment of normothermic brain temperature led to a virtually complete recovery of brain electric activity. The technique was suitable for investigations of ischemic and traumatic injuries [67].

2.5 Targeted volumetric cooling

Presently, only very limited volumetric cooling methods (VCM) are available. Through introduction of a cooling fluid into the target tissues, Ji and Liu established a VCM to selectively lower temperature of the target biological tissues [68]. In their approach, heat produced by cellular metabolism

can be directly transferred away by the cooling fluid (such as saline with lowered temperature), which was injected into the target from a syringe inserted into the tissues via a minimally invasive way. Both theoretical calculations and the *in vitro* and *in vivo* animal experiments indicated that VCM can significantly improve the cooling rate in the deep part of the tissues within a desired period of time, compared with that of surface cooling. This concept of VCM could also possibly be extended to wider clinical situations, where an instant and highly localized cooling for the specific organs or tissues is strongly requested. The expected cooling efficacy could be realized by controlling the flow rate and temperature of the coolant, the duration of an injection, or a combination of multiple syringes. A plausible merit of the VCM was in that it could achieve a rather rapid cooling for the specific region (such as deep part of tissue) under clinical emergencies, while other methods such as SBC, systemic body cooling or cold blood perfusion generally have to be performed for several hours, or even days, to achieve the target temperature. Besides, their operations are very complex and expensive. However, additional studies are still needed to get more comprehensive understandings on the physical as well as chemical representations of the VCM.

2.6 Side-effects of inappropriate cooling

Although brain cooling has been found un-replaceable for a high recovery of brain injury, it also possibly induces side effects in some situations, which should serve as a caution in clinics. For example, although brain cooling is an essential component of aortic surgery requiring circulatory arrest, and inadequate cooling may lead to brain injury, contrary output was also reported. As was shown, while normothermic CPB resulted in improved cardiac outcome, patients did not benefit from hypothermia-mediated brain protection and might be at high risk from ischemic brain injury [69]. In some studies, fatal cardiac arrhythmias were found to develop in the cooled heart [61]. Researches supported the idea that maintenance of normothermia during CPB might have advantages over hypothermia but there was a potential increased hazard of neurological injury [70]. Aortic cannula might allow simultaneous brain cooling during maintained corporeal normothermia. Fuller et al. used implanted miniature data loggers and fine thermistors to measure arterial blood and brain temperatures in four female pigs [71]. The results showed that SBC was present in pigs, but there was no clear relationship between blood temperature and the magnitude of SBC. Instead, the degree of SBC in pigs was governed by non-thermal factors, especially those associated with high sympathetic nervous system activity. Their results supported the concept that SBC might not always serve to protect the brain from thermal damage during heat stress.

It is now clear that whole-body cooling, adopted in the treatment of various brain pathologies [72], has limitations primarily because of management problems and severe side

effects (such as pneumonia) [64]. Potential complications include hemodynamic instability, coagulation disorders and infection. Instead, SBC appears to make good sense. Iatrou et al. investigated the effect of topical application of cool irrigation fluid on brain tissue temperature during craniotomy [73]. It was found that cooling the brain had a marked protective effect after brain injury, but systemic hypothermia could produce significant harmful effects. Their study demonstrated that the use of cool irrigation fluid during neurosurgery was a simple and effective method of cooling the brain while minimizing the use of systemic hypothermia. Further, it was also found that a cannulation system segmenting the aorta allowed independent control of cerebral and systemic perfusion. Such approach could provide significant cerebral protection while maintaining the advantages of warm systemic cardiopulmonary bypass temperatures [74].

Overall, enhancing the therapy output while minimizing the side-effects of brain cooling is still a big challenge for both clinicians and engineers.

2.7 Temperature monitoring for brain cooling

Monitoring brain temperature is rather important for evaluation and control of the hypothermia resuscitation process. Conventional monitoring sites may not reflect the core brain temperature. Kaukuntla et al. compared jugular bulb venous temperatures during deep hypothermic circulatory arrest and normothermic bypass with nasopharyngeal, arterial inflow, oesophageal, venous return, bladder and orbital skin temperatures [75]. It was found that during rewarming, all peripheral sites underestimated brain temperature. Therefore, caution is required to avoid hyperthermic arterial inflow, which may inadvertently result in brain hyperthermia. In many published studies, surrogate measures of arterial blood temperature have been used, which has potential to confound proper identification of SBC. However, Maloney et al. suggested that, using rectal temperature as a surrogate for arterial blood temperature did not provide a reliable indication of the status of the SBC effector [76]. Further, directly measuring brain temperature showed poor concordance between brain temperature and temperatures at other sites [41]. To be assured of achieving a desired brain temperature in any patient, some study suggested that at least three “central” sites (nasopharynx, esophagus, tympanic membrane, pulmonary artery) should be monitored. However, even this is still not guaranteed. Computer modeling indicates that brain cooling during CPB is principally determined by the temperature of the blood perfusion in the brain, cerebral blood flow, and the time allowed for cooling. The validity of using tympanic temperature as an index of brain temperature was also proposed [77], which seemed to be a good index for the core thermal inputs to the hypothalamic regulatory system, since variations in that parameter were associated with similarly directed variations in the sweating outputs [58]. In brief, establishing a good temperature index during brain cooling remains to be a problem in the near future.

3 Modeling of heat transport

3.1 General strategies

To numerically simulate the thermal behavior of the head subject to different cooling and thus to reveal its effect on the oxygen transport in the cerebrovascular network during circulation arrest, establishing a mathematical model is the first step. It should be pointed out that, complexity always exists when modeling the brain hypothermia. For example in cats, the behavioral state-dependent negative correlation of the pontine-hypothalamic temperature difference (an indicator of SBC), with the hypothalamic-ear pinna temperature difference (an indicator of heat loss from the heat exchangers of the head), is suppressed after bilateral common carotid ligature [31]. Behavioral state-dependent SBC may underlie a thermal feedback mechanism differentiating the relative influences of hypothalamic and extra-hypothalamic thermoreceptors on the thermoregulatory system during quiet wakefulness. Clearly, for a feasible modeling, some complexities will have to be approximated. Up to now, in nearly all the previous theoretical efforts, the thermoregulation mechanisms of the biological bodies have been neglected for simplicity. Therefore, the following discussion also falls into such category.

As is well known, arterial temperature decreases due to conduction of heat from the arterial blood to the surrounding tissue, and in the capillary bed the condition of very slow flow with a superposed oscillating component favors almost complete thermal equilibrium between the bloodstream and the surrounding tissue. Since the precapillary and capillary beds are the major sites for the exchange of heat in tissue, it is reasonable to assume the equality in postcapillary blood and brain tissue temperatures. Generally, due to highly nonhomogeneous thermal properties and perfusion rate from the interior of the brain to the skull, it is extremely difficult to quantify the thermal behavior of the brain by means of distinguishing the temperature in local tissue from the vascular network and the skull. Therefore, a simple and intuitive way is to introduce the temperature T to characterize the overall thermal state in a specific position of the head.

The well known Pennes equation has been commonly adopted as the best practical approach for modeling bio-heat transfer. This is because most of the other models still lack sound experimental basis and are generally very complex. Therefore, in view of its simplicity and wide applicability, the Pennes equation is being proved as a good candidate for characterizing the heat transport behavior in the skin tissues, and its general expression reads as

$$\rho c \frac{\partial T}{\partial t} = \nabla \cdot k \nabla T + \omega_b \rho_b c_b (T_a - T) + q_m \quad (1)$$

where, ρ , c , and k denote density, specific heat and thermal conductivity of tissue; ρ_b , c_b are density, specific heat of blood; ω_b is blood perfusion rate and can generally be

measured through a thermal clearance method; Q_m is metabolic heat generation; T_a is the supplying arterial blood temperature and T is the tissue temperature.

To model heat transfer in the brain subject to cooling, a spherical geometry is often used to represent the head, although a real anatomical geometry can also be processed. An improved, more complete modeling can be done in such a way that the brain is treated as consisting of several layers of cerebrospinal fluid, skull, scalp and brain tissues [20,78]. The geometric shape, dimensions, thermal properties and physiological characteristics for each layer, as well as the arterial blood temperature, can be used as the input to Pennes equation for a parametric study. Heat transfer equations from one to three dimensions have been analyzed.

Using such model and its extended expression, many issues concerned in the brain cooling can be tackled. For example, when cerebral circulation is hindered, which is a transient state, the blood perfusion may gradually reduce to zero in a short period of time, but the brain metabolism still continues until it runs out of the metabolic substrate. In such cases, Eq. (1) should be modified by incorporating these properties, although completely characterizing them is still a difficulty. For simplicity, the ischemic region of the brain can be reflected by reducing the blood perfusion rate to a lowered value or certain percentage of its normal value [20]. In some studies, the heat transfer term due to blood perfusion in Eq. (1) was even particularly omitted [44]. Instead, its effect was attributed to the heat conduction alone, which is also a routine procedure in modeling the bioheat transfer problem. Trezek and Jewett modeled and measured the transient temperatures in the brains of anesthetized cats and rabbits due to localized cooling to 5°C with probes of two different shapes [79]. Their results indicated that for the experimental conditions, metabolic heat and blood flow could be adequately accounted for by means of a rather small adjustment of the thermal diffusivity term in a general diffusion equation, without need of an explicit term for such distributed sources. Clearly, tremendous effort should be made to completely understand the role of blood perfusion in heat transfer during brain hypothermia resuscitation.

Another tough task in modeling brain cooling is to evaluate the metabolic heat generation, which depends on local brain temperature and time. The baseline metabolic rate is chosen as the rate which enables the patient to maintain his own body temperature in a normal state [80]. The most widely adopted approach in estimating the metabolic term has been to set it as the product of the oxygen consumption and its caloric value. But this is based on the assumption that oxygen, and not glucose, determines heat generation in tissues, which is improper for the ischemic situation. During circulatory arrest, the metabolic rate decreases with that of the local temperature. It is assumed that the metabolic rate changes according to the temperature coefficient, ϕ . On the other hand, the metabolism does not end until the substrate is depleted. Then one can assume that it decreases exponentially

with time [81], one of whose forms can be established as follows

$$Q_m(r, t, T) = Q_{m0} \cdot \phi^{[T(r, t) - 37]/10} \cdot \exp(-t / \tau_0) \quad (2)$$

where, Q_{m0} is the reference metabolic rate at 37°C, τ_0 is reference time at 37°C and is estimated as 300 s in some study. According to references [1,7,18], ϕ is set as 3.0.

It should be pointed out that few models have been developed to quantitatively investigate the effects of cerebral temperature changes during circulatory arrest on the oxygen consumption and how long could the patients withstand the oxygen delivery deficiency until all adenosine triphosphate (ATP) stored are depleted. However, such efforts will help achieve a better cooling approach to improve the patient's ability to survive in the hypoxia. Clearly, if combining the bioheat equation and the oxygen transfer equations together, the oxygen consumption dynamics can then be investigated. This will be explained later.

3.2 Theoretical evaluation of brain cooling effect

Many calculations that examine the effect of surface cooling on the head temperature development indicate that near the interior of the head, the temperature increases slightly at the beginning of circulation arrest [44]. This mainly resulted from an unbalance between the metabolic heat generation and the weak blood perfusion cooling. Such phenomenon was in fact reported in the past through experiment. Simulation showed that, temperature near the interior of the head decreased much more slowly than that of the skull surface. Even after a long period of time (say about 60 minutes), it still remained at a high level such as 36°C. Overall, the effect of surface cooling on the deep region was not evident, which was consistent with previous clinical data [7]. In some studies, SBC of varying strengths was demonstrated in a number of mammals and appeared to play a role in systemic thermoregulation. Nelson and Nunneley presented a mathematical model to explore whether surface cooling could effectively control the temperature of the human cerebrum [78]. It was found that cerebral temperatures were generally insensitive to surface conditions (air temperature and evaporation rate), which affected only the most superficial level of the cerebrum. The low surface-to-volume ratio, low tissue conductivity, and high rate of cerebral perfusion combined to minimize the potential impact of surface cooling, whether by transcranial venous flow or by conduction through intervening layers to the skin or mucosal surfaces. The dense capillary network in the brain assures that its temperature closely follows arterial temperature and is controlled through systemic thermoregulation independent of head surface temperature. Møllergaard [82] and Olsen et al. [43] also demonstrated that isolated head cooling, whether using frozen liquid or a cooling helmet, had a very limited effect on lowering the brain temperature.

Xu et al. developed a two-dimensional mathematical model to estimate the contributions of the following two

different mechanisms of brain cooling during cold-water near-drowning [80]: (1) conductive heat loss through tissue to the head surface and in the upper airway and (2) circulatory cooling to aspirated water via the lung and venous return from the scalp. Calculations indicated that conductive heat loss through the skull surface or the upper airways was minimal, although a small child-sized head would conductively cool faster than a large adult-sized head. However, ventilation of cold water through circulatory paths might provide substantial brain cooling. Although it seemed that water breathing was required for rapid "whole" brain cooling, it is possible that conductive cooling may also provide some advantage by cooling the brain cortex peripherally and the brain stem centrally via the upper airway [80]. Diao et al. developed a three-dimensional model to examine the transient and steady state temperature distribution in the brain during SBC and subsequent rewarming [83]. For the SBC induced through either wearing a cooling helmet or packing the head with ice, results suggested that the thermal contact between the head surface and the coolant in most commercially available cooling helmets was a main reason for delayed cooling in SBC as compared to the ice packing. Dexter et al. numerically analyzed the direct effects of haemodilution on the rate of brain cooling during cardiopulmonary bypass by analyzing changes in the blood's thermal properties [22,23]. A bioheat transport model was employed to predict the proportional direct effect of changing blood density and specific heat on the amplitude of the brain cooling rate. It indicated that within the haematocrit range used clinically during bypass, haemodilution with these substances had only a small direct effect on the rate of brain cooling. Vietla et al. applied the bioheat transfer equation to the analysis of intracranial temperature distributions [84]. The brain was isothermal at steady state, for perfusion rates of 1.0 and 0.1 mL/(mg·min⁻¹). The largest temperature gradients were observed in the nasopharyngeal (N-P) region. Altering surface heat transfer coefficient had little influence on brain temperature, even in regions of surgical exposure. Transient analysis demonstrated prompt reductions in cerebral temperature, with a slower fall in N-P temperature. Maintaining normal tissue perfusion throughout the cooling period ensured uniform temperature within the cerebral tissues and avoided inadequate local cooling arising out of ischemic insult. Sukstanskii and Yablonskiy proposed an analytical model of human brain temperature regulation [85]. The model described the distribution of brain temperature as a function of internal and external parameters, such as temperature of the incoming arterial blood, blood flow, oxygen consumption rate, ambient temperature, and heat exchange with the environment. It was shown that substantial changes in human brain temperature could be accomplished only through changes in the temperature of the incoming arterial blood or substantial suppression of blood flow. Other parameters could lead only to temperature changes near the brain surface.

Zhu evaluated the capacity of the heat loss from the carotid artery in human neck by establishing a model capable

of describing the effects of blood flow rate and vascular geometry on the thermal equilibration in the carotid artery [35]. It was shown that SBC existed in humans during hyperthermia, and the cooling of the arterial blood could be as much as 1.1°C lower than the body core temperature. The relative contributions of countercurrent heat exchange and radial heat conduction to SBC were comparable with each other. Taking into account an anatomically correct realistic 3-D head and neck with realistically varying local tissue properties, Dennis et al. developed a finite element model for the bioheat transfer in a human head subject to external cooling [86]. Effects of cold blood perfusion were calculated by considering several arterial temperatures for the perfusion cases. It indicated that rapid cooling of the brain in the first few minutes following the onset of cerebral ischemia is a potentially attractive preservation method. The criterion of successful cooling was taken to be the attainment of a 33°C average brain temperature within 30 min of treatment. For the cooling approaches of using ice packs applied to the head and neck as well as a head-cooling helmet, it was found that neither of these cooling approaches satisfied the 33°C temperature within 30 min. The authors suggested that substantial cooling could be achieved in conjunction with neck cooling if the blood speed in the carotid artery was reduced from normal by a factor of 10. Additional cooling means such as cooling of other pertinent parts of the human anatomy should be explored.

3.3 Modeling of VCM

As an alternative way to traditional methods, injecting cold fluid into the target to cool the tissues was recently proposed by Ji and Liu, which would induce an immediate temperature depressing effect [68]. Such VCM can be characterized by a two-phase porous medium flow and heat transfer model. When approximately treating the transport process in a one-dimensional spherical coordinate, the energy-balance equation for liquid in a transient state within a saturated two-phase porous medium can be written as [68,87,88]

$$\varepsilon_0 c_f \rho_f \frac{\partial T_f}{\partial t} + c_f \rho_f \varepsilon_0 \vec{u} \cdot \nabla T_f = \nabla [k_f \varepsilon_0 \cdot (\nabla T_f)] + h(T_t - T_f) \quad (3)$$

For the tissue phase in the porous medium, the energy-balance equation is similarly given as follows, where the well-known Pennes' blood perfusion term has been incorporated

$$\begin{aligned} (1 + \eta\beta)(1 - \varepsilon_0)\rho_t c_t \frac{\partial T_t}{\partial t} &= k_t(1 - \varepsilon_0) \frac{1}{r} \frac{\partial^2 (rT_t)}{\partial r^2} \\ &+ c_b w_b (Q_m)(T_a - T_t) + h(T_f - T_t) + Q_m(T_t) \\ &+ (1 - \eta)\beta c_f \rho_f (T_f - T_t) \end{aligned} \quad (4)$$

where, ρ_f is the density of fluid; u the velocity of fluid; T_f the temperature of the liquid phase; β fluid absorption rate per unit tissue volume; ε_0 for either volumetric or area porosity; c_f

the specific heat of fluid; k_f the thermal conductivity of liquid; h the volumetric heat convection coefficient between liquid and solid phases; T_t the solid tissue temperature; ρ_t , c_t , k_t are density, specific heat and thermal conductivity of the solid phase, respectively; and c_b is specific heat of blood. In reality, the fluid absorbed by tissues will not completely return to the venular blood. In other words, part of the liquid, called "stagnant fluid", stays in the tissue. The ratio of "stagnant fluid" to the whole absorbed-fluid is defined as η , %. The first term on the left of Eq. (4) includes the contribution of stagnant fluid to the solid phase's internal energy. While the fifth term on the right gives the heat loss due to the remaining liquid returning to the venular blood.

For the tissues unsaturated by fluid, heat is transported via conduction and blood perfusion, so the governing equation can be represented by the Pennes bioheat equation

$$c_t \rho_t \frac{\partial T_t^*}{\partial t} = k_t^* \frac{1}{r} \frac{\partial^2 (rT_t^*)}{\partial r^2} + \omega_b c_b (T_a - T_t^*) + Q_m(T_t^*) \quad (5)$$

where T_t^* and k_t^* are the temperature and the thermal conductivity of unsaturated tissues, respectively.

The fluid will gradually penetrate the tissues and get completely absorbed at a certain distal endpoint. The positions for the moving interface r_{int} can be determined using the mass conservation law. For example, if the cooling fluid flows out with a given velocity u_0 from the tip of a syringe at radial position r_0 , the transient position for the moving interface can be obtained as [68]

$$r_{\text{int}} = \left\{ r_0^3 + \frac{3u_0 r_0^2 \varepsilon_0}{\beta} [1 - \exp(-\beta t / \varepsilon_0)] \right\}^{1/3} \quad (6)$$

From this relation, the maximal saturation distance r_{max} for the cooling fluid, where flow rate is equal to zero, can be obtained as

$$r_{\text{max}} = \left(r_0^3 + \frac{3\varepsilon_0 u_0 r_0^2}{\beta} \right)^{1/3} \quad (7)$$

Using Eq. (6), the velocity for the moving interface is expressed as

$$\begin{aligned} u_{\text{int}} = \frac{dr_{\text{int}}}{dt} &= \left\{ r_0^3 + \frac{3u_0 r_0^2 \varepsilon_0}{\beta} [1 - \exp(-\beta t / \varepsilon_0)] \right\} \\ &\cdot u_0 r_0^2 \exp(-\beta t / \varepsilon_0) \end{aligned} \quad (8)$$

Solving Eqs. (3)–(5) satisfying the specific boundary and initial conditions would yield the tissue temperature distributions during fluid injection cooling.

3.4 Modeling heat and water transport in the respiratory tract

As a naturally existing path for cooling the brain, air flow across the respiratory tract also plays an important role in

In a vascularized biological tissue, blood flow plays an important role in the local transport of oxygen, nutrients, pharmaceuticals, waste products and heat through the body. However, this feature is often too complex to be quantified in modeling the oxygen transport. The Krogh tissue cylinder model of oxygen transport has served as the foundation and start point in this area for over 80 years [92]. It assumed that oxygen is exchanged between the parallel, evenly spaced capillaries and tissue. Based on it, a systematic analysis of oxygen transport in the brain was performed by Knisely et al. [93], using the numerical finite-difference method. However, anatomical data showed that the Krogh vessel configuration was not applicable to various organs. Therefore, other models with non-Kroghian geometry reflecting the morphological structure of specific tissues were also developed [94–96]. Several mathematical models for precapillary and postcapillary transport indicated significant amounts of oxygen exchange between arterioles and the surrounding tissue [10,97–99]. There were also discussions of the possibility of countercurrent exchange of oxygen between paired arterioles and venules [100–105]. Of the many existing oxygen transport models, only very limited researches took into consideration the anatomical vascular geometry. Disagreements among the theoretical predictions and the experimental measurements were therefore common in those studies. This was because geometrical irregularity of the vascular structure remained to be a major obstacle for the accurate modeling. Goldman and Popel proposed a computational model for oxygen transport from capillary networks [106]. This model was able to characterize the effect of complex geometry on oxygen transport. However, application of this model relied heavily on complicated calculations and the detailed construction of databases of anatomical and physiological data, which might lower the practical value of the method. It is for this reason that establishing a quantitative model, which is mathematically tractable in the region of interest and considering the detailed anatomical vascular geometry, has been a desirable objective. For this aim, Liu et al. [107,108] proposed a theoretical route through an analogy between the heat and mass transport modeling, to develop the basic equations for quantifying the oxygen transport inside a vascularized tissue. Having collectively included the contributions of the vascular geometry and the blood flow condition, their models provide a good theoretical prediction on previous experimental observations. Some typical features on such models will be illustrated in later sections.

Except for the above efforts, other models have also been formulated to reflect the heterogeneity of capillary architecture and hemodynamics in the brain [103,109]. For example, Ivanov et al. [109] studied the distribution of oxygen partial pressure (PO_2) in a microvascular unit composed of a spindle-shaped neuron surrounded by two capillaries. Through a different approach, the compartmental model ignoring the spatial variation dealt with exchanges between domains, called compartment, with a single value of concentration

assigned to each compartment [110,111]. Sharan et al. [112] modified the compartmental model of Roth et al. [113] and applied it to study oxygen transport in the brain including transport in the pre- and postcapillary microcirculation. This model was convenient to simulate the oxygen delivery in a system composed of many vessels and the tissue, because it ignored the spatial variation of variables in each compartment containing the lumped parameters and dealt with a single value of PO_2 assigned to each compartment. Ye et al. [114–116] modified and extended it to the oxygen-carbon dioxide coupled transport in the microcirculation involving the O_2 -Hb reaction kinetics and the Fåhræus effect. Of existing compartmental models for oxygen transport, few have taken into consideration of the effect of hemodynamic factors on the transient oxygen transport in the case of circulatory arrest. Only Sharan et al. [111] and Ye et al. [117] studied the cerebral blood flow under three different types of hypoxia without considering the variation of hemodynamic parameters. In order to have a better insight into the role of cerebral blood flow in regulating the PO_2 in microcirculation, a model for simulating the transient blood flow, which contained the variations of vessels in arteriolar compartments, the blood flux penetrating between the vessels and the surrounding tissue should be constructed.

4.2 Oxygen transport in cell level

As core elements of the brain, neurons, or nerve cells play a central role in storing and transferring information. In neurons, oxygen is closely related to the synthesis, metabolism, release and uptake of neurotransmitters [118]. Previous studies have shown that 40%–50% of the total adenosine triphosphate (ATP) produced in nerve tissue is used for neuronal activities. It is for this reason that oxygen supply and consumption dynamics have in fact been extremely important issues in cell biology. Research performed in Ref. [119] suggested that Down's syndrome neurons had a defect in the metabolism of reactive oxygen species that caused neuronal apoptosis. The hippocampal has been used for the investigation of neuronal damage during oxygen deprivation for a long time [120]. Hypoxia induces apoptosis and changes neuron cell cycle. Experiments have suggested that hypoxic preconditioning of animals in vivo increases hypoxic tolerance of hippocampal neurons [121–125].

The main body structures of neurons are in common with other cells, but the dendrites and axon make them unique. The neuron has a star-like appearance, with numerous long arms radiating out from its central cell body. Lv and Liu investigated the role of the dendrites and axon on oxygen transport over a neuron and suggested a mechanism to explain why a neuron is more easily damaged when subjected to insufficient oxygen supply, compared with other ordinary cell types [2]. In their model, the dendrites and axon were treated as 'fins' of the neuron, which turn out to enhance the oxygen transfer across the cell body. Then the transient

equation for the oxygen transport across these fins can be written as

$$\begin{cases} D \frac{\partial^2 C_i}{\partial x^2} + \frac{2\varphi}{r_i} (C_{\text{out}} - C_i) + g = \frac{\partial C_i}{\partial t} \\ C_i = C_b & x = 0, t > 0 \\ \frac{\partial C_i}{\partial x} = 0 & x = l_i, t > 0 \\ C_i = C_{i0}(x) & 0 \leq x \leq l_i, t = 0 \end{cases} \quad (12)$$

where D is diffusion coefficient of oxygen; C_i the transient oxygen concentration of dendrites/axon; C_{out} the surrounding oxygen concentration; g the oxygen consumed per volume and time in the soma.

For simplicity, the cell body-soma was treated as a solid sphere with radius $r = b$ having a uniform oxygen concentration over its sphere. Oxygen is consumed in the sphere at a constant rate of g . The oxygen concentration for the surroundings is prescribed at C_{out} . The lumped system model to characterize oxygen concentration in the cell body, can thus be established as

$$\frac{3\varphi(1-\gamma)}{b} (C_{\text{out}} - C_b) + g + \sum_{i=1}^{\text{nb}} \frac{3Dr_i^2}{4b^3} \frac{\partial C_i}{\partial x} \Big|_{x_i=0} = \frac{\partial C_b}{\partial t} \quad (13)$$

where nb is the number of the dendrites plus one axon, $S = 4\pi b^2$ the area of the cell body, $S_i = \pi r_i^2$ the cross-section area of the dendrites/axon, $V = 4\pi b^3/3$ the volume of the cell body,

$$\gamma = \sum_{i=1}^{\text{nb}} \frac{\pi r_i^2}{S}$$

the area density of the dendrites/axon versus the cell surface.

Calculations on the above model demonstrate that [2], existence of the dendrites and axon significantly enhances the oxygen transport to soma, which is beneficial for the neurons to maintain their normal functions. However, this function has dual opposite effects. When the surrounding oxygen concentration increases, the dendrites/axon serves to derive oxygen to the soma. However, in a hypoxic state, they also serve as a source for a neuron to quickly lose oxygen from its surface since multiple paths exist there. This will lower the levels of oxygen concentration in the neuron and appear as an adverse factor for the neuron to survive when subject to insufficient oxygen supply, such as in the case of blood circulation arrest.

4.3 Oxygen transport in vascularized tissues

Liu et al. [107,108] proposed a theoretical route to develop the basic equations for quantifying the oxygen transport inside a vascularized tissue. This basic idea starts from the analogy between the mass and heat transport modeling. The oxygen transport models thus established have collectively

included the contributions of the vascular geometry and the blood flow condition, therefore they can interpret well some previous experimental observations. Such theoretical route may provide a feasible way to comprehensively characterize the oxygen transport behaviors in living tissues with complex vasculature. It can also be extended to wider mass transfer issues such as drug and nutrients delivery, etc.

4.3.1 Pennes' perfusion term based model

For oxygen transport, the portion of oxygen consumed by the tissue arrives either directly from the arteriole, or by first diffusing into the capillaries to be dispersed to a much wider tissue region [126]. Such physiological behavior is similar to the role of blood flow in transferring heat. Therefore, in referring to the Pennes' equation form, a generalized oxygen transport equation using the blood perfusion term within biological tissues can be established as follows [107]

$$\frac{\partial C}{\partial t} = \nabla \cdot (D\nabla C) + \eta\omega_b (C_a - C) - R \quad (14)$$

where C_a and C are supply of arterial oxygen concentration and that of tissues, respectively; ω_b the blood perfusion rate; D the oxygen diffusion coefficient in living tissues; R oxygen consumption rate; η conversion efficiency ration coefficient. Since Eq. (14) is mainly used to describe the collective mass transfer effect for tissues not adjacent to large vessels, its predicted oxygen can thus not account for the directional convective mechanism of oxygen transfer due to blood flow.

Equation (14) can also be expressed in the form of oxygen partial pressure (or termed as oxygen tension) P as follows

$$\frac{\partial P}{\partial t} = \nabla \cdot (D\nabla P) + \eta\omega_b (P_a - P) - \frac{R}{\alpha} \quad (15)$$

where α is the solubility of oxygen. According to Henry's law, one can write the relation between the concentration of dissolved oxygen to the oxygen tension as $C = \alpha P$.

Subject to different coordinates, tissue types and clinical situations, various boundary and initial conditions for the above equation can be established. Solution to them will help understand the role of blood flow to the oxygen transport behavior. Some existing analytical approaches given before [127–130] can be applied to solve the above model.

A qualitative analysis on Eq. (14) can easily lead to the conclusion that the decrease of the blood perfusion will result in a low oxygen level in tissues, which reflects the case of physiological hypoxia state due to circulation arrest. It is possible that some pathological cause of hypoxia due to insufficient blood flow or circulation arrest can be tested along this way. Further, since the equation form of Eq. (14) has been extensively studied from the heat transfer aspect, further study on its value in modeling the oxygen transport can borrow ideas there. For example, studies have shown that vessels in the range of 50–500 μm diameter primarily contribute to tissue heat transfer in living systems [131].

Correspondingly, oxygen transport due to various vessel sizes also need to be investigated in detail. Besides, as has recently been demonstrated, capillaries are not the sole supplier of oxygen for tissue. Other microvessels also contribute to tissue oxygenation [126]. Therefore, a lot of fundamental issues need to be clarified in the near future.

4.3.2 Chen-Holmes model based oxygen transport equation

Following the same approach as illustrated above, and in analogy to the well-known Chen-Holmes bioheat equation [132], a new oxygen transport equation which has included contributions from both the blood perfusion and blood flow, can be established as follows [107]

$$\frac{\partial C}{\partial t} = \nabla \cdot (D + D_b) \nabla C + \eta \omega_b^* (C_a^* - C) - v_b \cdot \nabla C - R \quad (16)$$

where D_b denotes the enhancement of oxygen diffusivity in the tissue due to the flow of blood within blood vessels; v_b is velocity vector for blood flow; as exactly defined by the original Chen-Holmes' equation, C_a^* is the oxygen concentration of the arterial blood in the first generation that can be legitimately represented in the continuum model, the j th generation; similarly, ω_b^* is the blood perfusion rate only from blood vessels beyond the j th generation.

Several new terms appear in this mass conservation equation for a tissue control volume perfused by flowing blood. This equation appears more complete in including the effects of blood flow. However, it also increases the difficulty for the solution. Neglecting the second term on the right hand side of Eq. (16) would lead to the Wulff model [133]. An in-depth analysis on the applicability of Eq. (16) to model the oxygen transfer can be made by digesting the physiological meaning of the original Chen-Holmes' model, as has been comprehensively discussed by Chen and Holmes [132], and Charny [134].

4.3.3 Oxygen transport equation for tissues surrounding a large blood vessel

Oxygen transport in tissues surrounding a large blood vessel can be studied by using the coupled equations. For this purpose, Eq. (14) for oxygen transport in the perfused tissue and a diffusion-reaction equation for the oxygen concentration of flowing blood either in a single vessel or counter current vessel pairs can be combined to investigate the detailed oxygen delivery behavior, similar to the heat transfer analysis as performed before by Huang et al. [135] and Charny et al. [136].

4.3.4 W-J model based oxygen transport equation

Based on the conceptual microvascular structure of skin tissues proposed by Weinbaum, et al. [137] and Jiji et al.

[138], and in analogy to the well known W-J bioheat equation [139], Ji and Liu obtained a three-layer mathematical model to characterize the detailed oxygen transport in three geometrically distinct peripheral regions: deep tissue layer, intermediate layer and cutaneous layer, respectively [108]. For the deep tissue layer, the equation for the average oxygen transport (\bar{C}_t) reads as [108]

$$\frac{\partial \bar{C}_t}{\partial t} - \frac{\partial}{\partial x_i} \left[(D_{ij})_{\text{eff}} \frac{\partial \bar{C}_t}{\partial x_j} \right] = -R - \frac{\pi^2 n a^2 D_t}{4\sigma(\mu_1 + \mu_2)} P e_m^2 l_j \frac{\partial l_j}{\partial x_i} \frac{\partial \bar{C}_t}{\partial x_j} \quad (17)$$

where, the average oxygen concentration \bar{C}_t is introduced to characterize the oxygen transport in the layer, which can be defined by

$$\bar{C}_t = (1 - W)C_t + \frac{W}{2}(C_a + C_v)$$

reflecting the overall contributions of C_a , C_v and C_t in the vascular tissues; l_j is direction cosine; μ_1 , μ_2 are coefficients addressing the contributions of C_a and C_v to C_t , i.e., for the region with vessels, the average tissue oxygen concentration can be linearly approximated by $C_t \approx \mu_1 C_a + \mu_2 C_v$; σ is shape factor and related to the cross-sectional geometry by the relation $\sigma = \pi / \text{arc cosh}[l(s)/2a(s)]$. The dimensionless number $P e_m = 2au/D_t$ was named as mass Peclet number [108], which reflects the ratio of the oxygen transported via blood flow to that by diffusion in the tissue. The above equation has collectively included the contributions of the vascular geometry and the blood flow condition. The second term on the right-hand side of Eq. (17) results from the spatial variation of vessels diameter, number, and blood velocity, which is small and would vanish entirely if the countercurrent vessels were perpendicular to the x_i axis, since $\partial l_j / \partial x_i$ would become zero [140].

In Eq. (17), $(D_{ij})_{\text{eff}}$ indicates the effective diffusivity, which is

$$(D_{ij})_{\text{eff}} = D_t \left[\delta_{ij} + \frac{\pi^2}{4\sigma(\mu_1 + \mu_2)} n a^2 P e_m^2 l_j l_j \right] \quad (18)$$

where the second term in the parenthesis represents the enhancement on oxygen diffusion due to the countercurrent blood flow. For the one-dimensional case the blood vessels and the oxygen concentration gradient are in the same direction. Eq. (18) can then be expressed by:

$$D_{\text{eff}} = D_t \left[1 + \frac{\pi^2}{4\sigma(\mu_1 + \mu_2)} n a^2 P e_m^2 \right] \quad (19)$$

In the classical oxygen diffusion equation, the oxygen diffusion coefficient D_t was treated as the same regardless of the types of muscle and experimental conditions [141–145]

unless effects of vascular geometry and blood flow were considered. Ji and Liu [108] made an estimation in Fig. 2 on the magnitudes of the enhancement in tissue oxygen diffusion due to countercurrent vessel pairs with varying size (where $\mu_1 \approx \mu_2 \approx 1/2$ is assumed, the physiological parameters are from Ref. [146], the diffusion coefficient for unperfused tissues is applied as $D_t = 1.5 \times 10^{-5}$ cm/s [91], and the countercurrent vessels number density is fixed at 32 number/cm² [108]). It is shown that the larger the vessel diameter and blood velocity are, the greater the value of D_{eff}/D_t . Even for the vessel diameter $d = 50$ μm , the D_{eff} is still two orders of magnitude higher than D_t . For the terminal vessels with the much smaller diameter and lower blood velocity, further calculations show that the D_{eff} is much higher than D_t . All these results reveal that the effective diffusion coefficient D_{eff} reflects the average oxygen transport amplification by the countercurrent vessel convection, compared to pure diffusion by the tissue alone. Bearing the extremely high value of D_{eff} in mind, one can then understand well the cause that the experimentally measured oxygen loss from arterioles is usually orders of magnitude higher than previous theoretically predicted results [9,99]. Clearly, the vascular geometry plays an important role in oxygen transport in the perfused tissue.

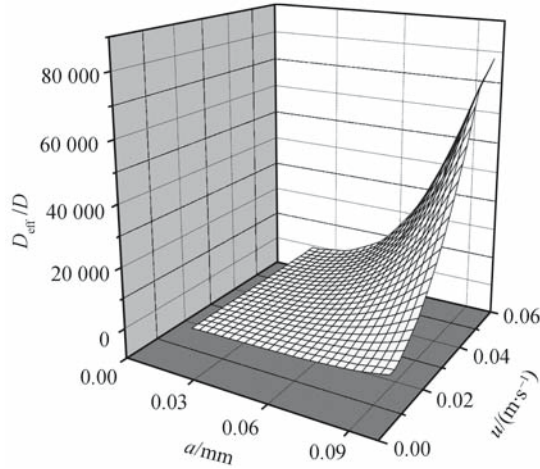


Fig. 2 The effective oxygen diffusivity profile under different blood flow velocities and vessel diameters

For the intermediate capillary layer (second layer), starting from the transverse terminal vessels, a periodic array, it first appears in the skeletal muscle tissue and extends to the interface with the cutaneous layer (the third layer) [137], a different equation from above should be developed to characterize the oxygen transport there. In general, the networks of terminal vessels deliver oxygen to capillary beds where they also diffuse oxygen to tissue. In earlier studies [91,99,147], researchers found that the spatial pattern of capillaries is one of many factors important for the description of oxygen tension in a specified region of tissue. In fact, a complex pattern of O₂ exchange exists among arterioles, venules, and adjacent capillary networks. In previous multicapillary

simulations of oxygen transport in skeletal muscle, two main approaches have been applied [10]. One is to assume that capillaries lie in a regular, evenly spaced array. The other is to distribute capillaries randomly and independently over the region. To focus on the effect of capillary beds on the average oxygen concentration distribution in the layer, one must consider the spatial pattern and the blood velocity in the capillary. For simplicity, Ji and Liu assumed a parallel and regularly spaced capillary pattern providing the distribution of oxygen over this tissue layer [108]. Applying the idea proposed by Salathe [147], a description of the fine-scale intercapillary variation is not necessary for an understanding of the overall manner in which oxygen is supplied to a given organ. An average oxygen concentration \bar{C}_t is introduced to characterize both tissues and capillaries.

Using porous medium mass transfer theory, a transient governing equation for the intermediate layer can be established as

$$\frac{\partial \bar{C}_t}{\partial t} = \nabla \cdot D_t \nabla \bar{C}_t - v \cdot \nabla \bar{C}_t - R \quad (20)$$

where v and R respectively represent the average capillary blood velocity and oxygen consumption rate. Eq. (20) allows one to solve for the oxygen distribution in this layer without calculating the details around an individual capillary.

The outermost layer is the cutaneous layer, which is supplied by a separate circulation of widely dispersed large vessels in the deep tissue that rise to the surface and feed the superficial arteries and veins in the cutaneous plexus. The microvascular structure described by Weinbaum et al. [137] suggested that the cutaneous layer is split into two regions, an inner region and outer region. The inner region can be described by ordinary diffusion differential equation, i.e.

$$\frac{\partial \bar{C}_t}{\partial t} = \nabla D_t \nabla \cdot \bar{C}_t - R \quad (21)$$

where \bar{C}_t denotes an average oxygen concentration as stated previously.

For the outer region, it has little metabolism, then the oxygen consumption can be neglected and the governing equation is given by

$$\frac{\partial \bar{C}_t}{\partial t} = \nabla D_t \nabla \cdot \bar{C}_t \quad (22)$$

As calculations shown in Ref. [108], the mass Peclet number Pe_m decreases with the increase of the distance from the tissue base. The variation of Pe_m is reflected on the effective diffusivity D_{eff} . Overall, the effective enhancement of the tissue diffusion is due to the vascular configuration. For much smaller diameter and lower blood velocity, results still indicate that D_{eff} can also be much higher than D_t (Fig. 3), which explains the experimental data that oxygen loss from arterioles is orders of magnitude higher than previous theoretical prediction [9,99].

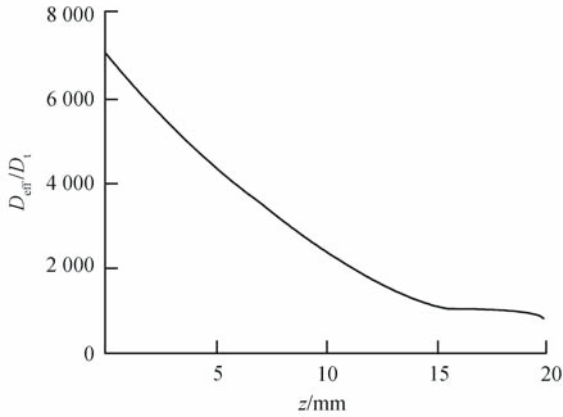


Fig. 3 D_{eff}/D_t varying with distance

From the above model, one can approximately evaluate the amount of oxygen exchange flux between the artery and vein $f_{a,v}$. The results indicate that, for the small blood velocity in deep tissue layer, the oxygen gradient $\partial \bar{C}_{t1}/\partial z$ becomes larger with the decrease of vessel diameter, so $f_{a,v}$ will be relatively larger than that of the case with higher velocity. For the high blood velocity, the oxygen concentration slowly decreases with the distance. Especially at the deepest region, its gradient $\partial \bar{C}_{t1}/\partial z$ appears close to zero even for a small blood velocity. Further calculations indicate that $C_a - C_v = f_{a,v}/\sigma D_t$ is generally several orders of magnitude smaller than \bar{C}_{t1} . Therefore, for the tissue areas with large blood vessels and relatively high blood velocity, the oxygen exchange between arterioles and venules can be omitted. This conclusion is strongly supported by a lot of previous experiments and theoretical studies [100–105, 148, 149]. Further, one can find that the average oxygen concentration is extremely uniform over the whole intermediate layer, which has been experimentally verified [98]. It is stated [98, 99, 150, 151] that for a given metabolic condition, the amount of oxygen loss from a capillary does not depend solely on the rate of capillary blood flow rate. It also relies on a combination of factors being strongly influenced by the proximity arterioles and venules (terminal vessels). Existence of diffusive interactions enables oxygen to be delivered to tissues more uniformly than it might be if there was only a convective source of oxygen from small terminal arterioles. Therefore, the diffusive interaction between capillaries and other microvessels still needs further considerations in the future. In the cutaneous layer, the average oxygen concentration decreases and inflow blood velocity has significant influence on the oxygen magnitude (Fig. 4). The concentration distribution in the outer region appears as a linear curve since no oxygen consumption occurs there. This is different from the case in the inner region with oxygen consumption.

In previous studies, although many theoretical models have been proposed to analyze the oxygen transport in living tissues, only very limited researches have simultaneously taken into account the vascular effects such as large artery,

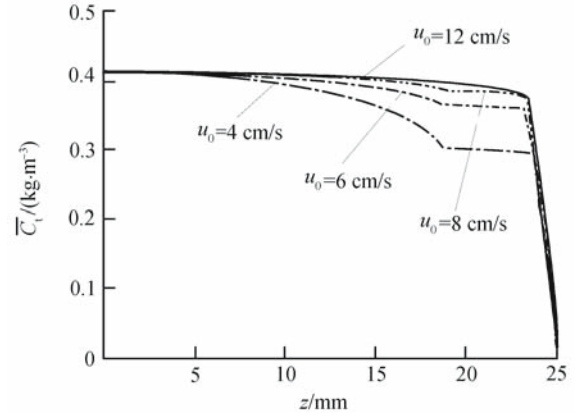


Fig. 4 Effect of blood flow velocity to average oxygen concentration

arterioles network, capillary, perfused-tissue or microcirculation [152–156], and oxygen concentration or partial pressure in different regions is usually treated individually. In most practices, one wishes to seek a simple variable to characterize the local oxygen transport and exchange. A plausible merit of the above models is that they possess a new idea from which one can explore the collective effects of vascular geometry and blood flow conditions on the tissue oxygen concentration. In such models, complexity of the vasculature with locally varying vessel size, number density, velocity and direction can possibly be taken into consideration via a much simpler way. The established equations are remarkably simple in linear differential form with spatially varying coefficients, which are prescribed as the functions of local vascular geometry and blood flow. Further, based on this research, one can still have additional insight into the oxygen transport process with varied physiological and pathological conditions. For example, transporting of CO_2 coupled with O_2 through the Bohr effect (effect of CO_2 tension on blood O_2 content) and the Haldane effect (effect of PO_2 on the blood CO_2 content) could be studied in this way.

4.4 Compartmental model for oxygen transport in brain tissues

4.4.1 Oxygen equation

As is gradually realized, simultaneously dealing with the transient behaviors of the cerebral blood flow over the whole vessel circuit and oxygen transport appears rather difficult if still using the distributed parameter model, as described before. This requests another completely different modeling approach, the so-called compartmental model. Such model is convenient to simulate the oxygen delivery in a system composed of many vessels and tissues, because it ignores the spatial variation of variables in each compartment containing the lumped parameters and deals with a single value of PO_2 assigned to each compartment. As shown in the schematic structure of Fig. 5 which was studied first by Sharan et al.

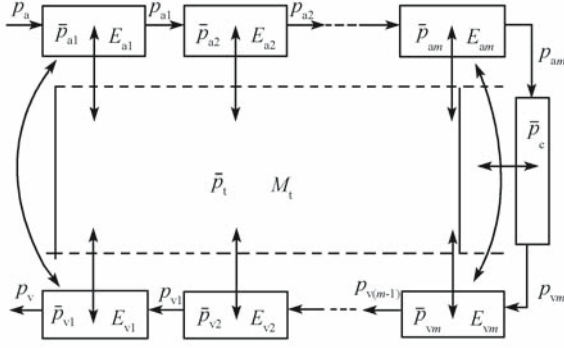


Fig. 5 Compartmental model for a brain microcirculatory unit

[112] and then extended to the brain cooling area by Ji and Liu [157], the vascular bed can be represented as a series of vascular compartments surrounded by a tissue compartment, which consists of m (a_1, a_2, \dots, a_m , number as $i = 1, 2, \dots, m$) arteriolar and m (v_1, v_2, \dots, v_m , number as $i = 1, 2, \dots, m$) venular compartments, and one capillary compartment. \bar{p} denotes oxygen partial tension in a compartment; E denotes diffusion conductance; and M is the rate of cerebral oxygen consumption. Arterioles (a_1, \dots, a_m) and venules (v_1, v_2, \dots, v_m) are classified into $2m$ compartments on the basis of vessel diameter [112]. Each compartment contains vessels of the same diameter and length, arranged parallel to each other. As blood flows through the vascular bed, oxygen is transported by convection in the vascular compartments and by free diffusion into the tissue where it is utilized. Also, oxygen is permitted to diffuse between the arterioles and venules at the same branch level in the process of countercurrent exchange. In this model, the influence of changed temperature on the thermally significant coefficients can be taken into consideration, which is to characterize the hypothermia effect on the oxygen transport and consumption behavior in brain during circulation arrest.

In Ji and Liu's work [157], a transient compartmental model was established to simultaneously quantify the dynamic blood flow (see Fig. 6) and the oxygen transport (see Fig. 5) along the cerebral vascular network during circulation

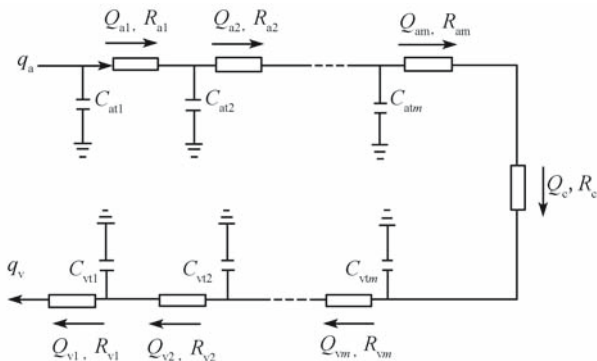


Fig. 6 Electrical analog of the cerebrovascular dynamics

arrest. The two models were then combined to analyze the transient blood flow and oxygen partial pressure (PO_2) distribution over the successive branches of vascular network, using the morphological and physiological data of animal brain. In this way, influences of the blood flow rate, the vascular diameter and the capacitive effect to the oxygen transport during circulatory arrest in patients with severe head injury can be investigated. In Fig. 6, (R_{ai} , C_{ai}) and (R_{vi} , C_{vi}) represent the lumped resistance, compliance of the cerebral arterioles and venules, respectively; q_a is the inlet arterial hydraulic pressure; q_v is the outlet venous hydraulic pressure.

The mass balance in a transient state for each of the vascular compartments can be established as follows [157]

$$Q_{ai}(C_{a(i-1)} - C_{ai}) - E_{ai}(\bar{p}_{ai} - \bar{p}_t) - F_{ai}(\bar{p}_{ai} - \bar{p}_{vi}) = \frac{\partial(V_{ai}\bar{C}_{ai})}{\partial t}, \quad i = 1, 2, \dots, m \quad (23)$$

$$Q_c(C_{am} - C_{vm}) - E_c(\bar{p}_c - \bar{p}_t) = \frac{\partial(V_c\bar{C}_c)}{\partial t} \quad (24)$$

$$Q_{vi}(C_{vi} - C_{v(i-1)}) - E_{vi}(\bar{p}_{vi} - \bar{p}_t) - F_{vi}(\bar{p}_{vi} - \bar{p}_{ai}) = \frac{\partial(V_{vi}\bar{C}_{vi})}{\partial t}, \quad i = 1, 2, \dots, m \quad (25)$$

where, C_{ai} is the oxygen content at the outlet of the i th arteriolar compartment, \bar{C}_{ai} is the averaged oxygen content in the i th arteriolar compartment and can be calculated as

$$\bar{C}_{ai} = (C_{a(i-1)} + C_{ai})/2$$

\bar{p}_{ai} and Q_{ai} are, respectively, the spatially averaged oxygen tension and blood flow rate in the i th arteriolar compartment, V_{ai} is the volume of the i th arteriolar compartment, E_{ai} and F_{ai} are the diffusion conductance or exchange coefficient for the i th arteriolar compartment, \bar{p}_t is the oxygen tension in the tissue, and $C_{a0} = C_a$ is the oxygen content in the blood entering the vascular network with the oxygen tension p_a . The subscripts "v" and "c" refer to the corresponding quantities in the venular and capillary compartments. \bar{p}_i represents the lumped oxygen partial pressure in the i th compartment, and p_a is the input arterial partial pressure of oxygen. E_i and F_i are the vessel-tissue diffusion conductance and the paired exchange coefficient for the i th vascular compartment. C_{vi} denotes the oxygen content at the inlet of the i th venular compartment and $C_{v0} = C_v$ is the oxygen content in the blood leaving the vascular network with the oxygen tension p_v . In each of Eqs. (23)–(25), the first term on the left represents the transport of oxygen by convection, the second term gives the transport of oxygen from the blood to the surrounding tissue, while the last term is due to countercurrent diffusional exchange between paired arterioles and venules. The term on the right represents the rate of accumulation of oxygen concentration. For simplicity, the chemical reaction between oxygen and hemoglobin can be assumed to be in equilibrium.

Therefore, the oxygen content in blood flowing out of the i th vascular compartment is expressed as [91]

$$C_i = \alpha_b p_i + \beta HS(p_i) \quad (26)$$

where α_b is the solubility of O_2 in the blood, p_i is the oxygen tension at the outlet of the i th compartment, H is the blood hematocrit expressed as a fraction of unity, S is the fractional saturation of hemoglobin with oxygen, and β is the oxygen-carrying capacity per unit volume of red blood cells. When a fraction of hemoglobin molecules is occupied by carbon monoxide, the coefficient β can be expressed as [91]

$$\beta = 1.34[\text{Hb}](1-\text{SCO})/H^o \quad (27)$$

where $[\text{Hb}]$ is the total hemoglobin concentration in grams per 100 mL of blood under control conditions, H^o is the blood hematocrit under normal conditions and SCO is the fractional saturation of hemoglobin with carbon monoxide.

The relationship between the fractional saturation of hemoglobin with oxygen, SO_2 , and oxygen tension is known as the oxyhemoglobin dissociation curve (ODC). In most of the physiological and clinical applications, the Hill equation is used to express ODC because of its simplicity, when cerebral circulation arrest occurs, hypoxia will be caused due to decreasing blood flow. The Hill equation cannot accurately describe the lower saturation. Thus, one can still use the fairly accurate Adair equation for SO_2 as a function of the oxygen tension and other parameters [91]

$$S = \frac{a_1 p + 2a_2 p^2 + 3a_3 p^3 + 4a_4 p^4}{4(1 + a_1 p + a_2 p^2 + a_3 p^3 + a_4 p^4)} \quad (28)$$

where, p is the partial oxygen pressure, and a_i ($i = 1, 2, 3, 4$) are the Adair constants, which can be calculated as $a_1 = 1.22 \times 10^{-2}$, $a_2 = 9.96 \times 10^{-5}$, $a_3 = 0$, and $a_4 = 3.96 \times 10^{-7}$ [158,159].

Recently, Ye et al. [114] have shown that the average oxygen tension \bar{P}_i within each noncapillary compartment can be better obtained by using an arithmetic average of inlet and outlet compartmental oxygen tension. For capillary compartment, the \bar{P}_c can be calculated by a logarithmic distribution. Therefore, the average oxygen tension in each vascular compartment can be expressed as [116]

$$\bar{P}_i = \xi_i (p_{i-1} + p_i) / 2 \quad (29)$$

where

$$\xi_i = \begin{cases} 1.2838 - 0.09513 \ln(p_{\text{am}}) & \text{capillary compartment,} \\ & p_{\text{am}} \geq 20 \\ 1.0 & \text{otherwise} \end{cases} \quad (30)$$

In the tissue compartment, the accumulation rate of O_2 is balanced by the net transport of O_2 by diffusion from the vascular compartments, and the consumption of oxygen in

the metabolic processes. The transient mass balance equation for the tissue compartment is established as [157]

$$\sum_{i=1}^m E_{ai} (\bar{P}_{ai} - \bar{P}_t) + E_c (\bar{P}_c - \bar{P}_t) + \sum_{i=1}^m E_{vi} (\bar{P}_{vi} - \bar{P}_t) - MV_t = \frac{\partial(V_t \bar{C}_t)}{\partial t} \quad (31)$$

where $\bar{C}_t = \alpha_t \bar{P}_t$ is the average oxygen concentration in the tissue compartment, and where α_t is the solubility of O_2 in the tissue. V_t is the volume of brain tissue, And M is the oxygen metabolic rate, which includes the temperature effect.

The parameters for the compartmental model of oxygen transport have to be specified before calculation. Sharan et al. [112] have derived the diffusion conductances and the countercurrent exchange coefficients. The compartmental model suggested the existence of the countercurrent diffusional exchange between all paired arterioles and venules. Previous studies predicted that only a small amount of oxygen diffuses from arterioles to venules [108,110,111]. The diffusion conductance E_i and exchange coefficients F_i for each vascular compartment of lamb brain can be found in the literature.

Sharan et al. [112] derived the diffusion conductances and the countercurrent exchange coefficients. Diffusion conductance for capillary compartment, in which they assumed the capillaries are the only source of O_2 and the axial diffusion of O_2 is negligible in comparison with the radial diffusion and excluded the radial diffusion resistance of intravascular blood as well as that of vessel wall and tissue, is given by

$$E_{c0} = \frac{4\pi N_c L_c D_t \alpha_t (1 - w^2)}{2/(1 - w^2) \cdot \ln(1/w) - (3 - w^2)/2} \quad (32)$$

where E_{c0} is the oxygen diffusion coefficient for capillary compartment at 37°C . N_c is the total number of capillaries and L_c is the length of the capillary. $w = r_c/r_t$ is the Krogh ratio of the capillary radius to the effective tissue cylinder radius. Because of those assumptions, Eq. (32) overestimates the value of diffusion conductance for capillary compartment, Ye et al. [115] presented a more accurate expression to calculate it. For the non-capillary compartment, the derivation of diffusion conductance E_i differs from that of capillary E_c . Based on an earlier model in which the influence of the vessel wall and a tissue layer with a fixed penetration depth l_t were taken into account [108,110,111], the diffusion conductance E_i for each arterial or venular compartment of sheep brain at normal state can be calculated.

4.4.2 Blood flow equation

In order to calculate the transient oxygen tension distribution across the vascular compartments and tissue compartment, the unknown hemodynamic parameters, $Q_{ar/vi}$, Q_c contained in Eqs. (23)–(25) need to be determined in advance. For this purpose, a transient compartmental model for blood flow

behavior was developed [157], which is geometrically in accordance with the oxygen compartmental model.

In steady state [111,112,115,116], blood flow was treated as proportional to the pressure drop along the flowing passage, i.e., $Q = (q_{in} - q_{out})/R$, where q_{in} , q_{out} and R are inlet hydraulic pressure, outlet hydraulic pressure and resistance, respectively, which are treated as constant. Modeling of transient blood flow behavior requires dealing with more factors than that in steady state.

During circulatory arrest, the cerebral arteries are under control by many regulatory mechanisms that act on the vascular bed to maintain an adequate cerebral blood flow. These mechanisms regulate the arterial vessels by modifying their radius, and thus altering the CBF. As demonstrated by the previous literatures [160–164], several distinctively different factors work on the cerebrovascular network, which might represent production of chemical substances by cerebral tissue during hypoxia and their vasodilatory effect on arterial vessels (chemical mechanism), direct response of smooth muscle to stress (myogenic mechanism), or effect of neural vasomotor fibers on the caliber of proximal cerebral vessels (neurogenic mechanism). Myogenic mechanism can be incorporated to characterize the transient blood flow. Ursino et al. [160–162] investigated the role of tissue hypoxia in cerebrovascular regulation. They found that only the medium and small arteries and the arterioles were under the action of these chemical substances during hypoxia. In fact, chemical agents could not easily reach the larger arteries through diffusion. It is very difficult to construct a simple and direct mathematical model to describe the effect of chemical mechanism on the vessel dilation.

The cerebrovascular system can be simulated through a resistance-compliance circuit as shown in Fig. 6. The vascular tree is also divided into five arteriolar segments (a_1, a_2, \dots, a_m , number as $i = 1, 2, \dots, m$) and five (v_1, v_2, \dots, v_m , number as $i = 1, 2, \dots, m$) venular segments, and one capillary segment. Each segment, in which the vessels have the same diameter and length as that of each compartment in the oxygen transport model, represents a generation of vascular tree. (R_{ai} , C_{ai}) and (R_{vi} , C_{vi}) correspond to the lumped resistance, and the compliance of the i th arteriolar or i th venular segment. R_c is the lumped resistance of the capillary segment. q_a is the arterial hydraulic pressure entering the network; q_v is the venular hydraulic pressure leaving the vascular network. The continuity equations for the mass balance of each segment can be expressed as:

for arteriolar segment

$$\frac{q_{a(i-1)} - q_{ai}}{R_{ai}} = \frac{q_{a(i-2)} - q_{a(i-1)}}{R_{a(i-1)}} - C_{ai} \frac{dq_{a(i-1)}}{dt} \quad (i = 2, 3, \dots, m) \quad (33)$$

for capillary segment

$$\frac{q_{am} - q_{vm}}{R_c} = \frac{q_{a(m-1)} - q_{am}}{R_{am}} \quad (34)$$

for venular segment

$$\frac{q_{vm} - q_{v(m-1)}}{R_{vi}} = \frac{q_{am} - q_{vm}}{R_c} - C_{vm} \frac{dq_{vm}}{dt} \quad (35)$$

$$\frac{q_{vi} - q_{v(i-1)}}{R_{vi}} = \frac{q_{v(i+1)} - q_{vi}}{R_{v(i+1)}} - C_{vi} \frac{dq_{vi}}{dt} \quad (i = 1, 2, \dots, m-1) \quad (36)$$

where q_{ai} is the blood hydraulic pressure at the outlet of the i th arteriolar segment and $q_{a0} = q_a$, q_{vi} denotes the blood hydraulic pressure at the inlet of the i th venular segment. $R_{ai/vi}$ and R_c is the lumped resistance of the i th vascular segment and capillary segment, respectively. $q_{v0} = q_v$ approximates to zero. In each of the equations for vascular segments, i.e. Eqs. (33)–(36), the first term on the left represents the transport of blood via convection in the i th segment, the first term on the right gives the transport of blood by convection in the upstream segment, the second term on the right is introduced on considering the capacitive effect. The capillary is considered as non-deformed, therefore, no compliance exists there.

Since the Reynolds number characterizing the cerebrovascular flow is very small, the blood flow can be assumed as a fully developed laminar pipe flow. According to the well-known Poiseuille law, the hydraulic resistance in each vascular segment is given by [112]

$$R_{ai/vi} = \frac{\eta L_i}{N_i d_i^4 (\bar{q}_{ai/vi})} \quad (i = 1, 2, \dots, m) \quad (37)$$

where, $\eta = 128\mu_{pl}/\pi$. L_i is the characteristic length of vessels, N_i is the number of vessels in the i th vascular segment. μ_{pl} is the plasma viscosity, assumed to be constant. The vessel diameter d_i in the i th vascular segment depends on the average intravascular pressure $\bar{q}_{ai/vi}$ in the segment, which can be treated as $\bar{q}_{ai/vi} = (q_{a(i-1)/v(i-1)} + q_{ai/vi})/2$. The capillary resistance R_c can also be calculated in terms of Eq. (37).

It is desired to model the relationship between the variation of arterial vessels caused by myogenic response and the local intravascular pressure during circulatory arrest. Cavalcanti and Ursino [163] suggested a model for the pressure-dependent diameter changes, which is derived by distinguishing the passive and viscoelastic response of the arterial wall from the active response caused by myogenic reflex (the increase of vascular wall tension caused by a rise in blood pressure intensifies the smooth muscle activity, thereby eliciting a sustained vessel constriction). This proposed approach can be applied in the simulation. Therefore, the pressure-dependent arteriolar diameter can be expressed as the sum of an elastic deformation, d_e and a myogenic contraction d_m [163]

$$d_{ai}(\bar{q}_{ai}) = \sigma_{ai} [d_{ei}(\bar{q}_{ai}) + d_{mi}(\bar{q}_{ai})] \quad (i = 1, 2, \dots, m) \quad (38)$$

where σ_{ai} is a shape factor, which depends on the vessels of branch level. The arteriolar elastic deformation exhibits an

exponential behavior. Therefore, the elastic deformation in the passive state can be expressed as [163]

$$d_{ei}(\bar{q}_{ai}) = d_0 + g\bar{q}_{ai} + \delta\left[1 - \exp(-\gamma\bar{q}_{ai})\right] \quad (i = 1, 2, \dots, m) \quad (39)$$

where, d_0 is the undeformed vessel diameter ($\bar{q}_{ai} = 0$); g , δ , γ are the constant coefficients. When the myogenic reflex becomes active, the active contraction is modeled through an empirical expression [163]

$$d_{mi}(\bar{q}_{ai}) = \frac{a - \sqrt{b + c\bar{q}_{ai}}}{1 + f_1 e^{2\bar{q}_{ai}} + f_2 e^{\beta\bar{q}_{ai}}} \quad (i = 1, 2, \dots, m) \quad (40)$$

The parameters in Eqs. (39) and (40) can be found in Ref. [163].

The vessels of arterial segments exhibit an evident myogenic activity during circulatory arrest. Therefore, their diameters are regulated according to Eqs. (38)–(40). For the capillary, vessel diameter is too small to be able to exhibit myogenic activity, thus the resistance R_c is kept constant. The resistance neglecting the vasomotion simulates the postcapillary circulation. When circulation arrest occurs, production of chemical substances during hypoxia (i.e., chemical mechanism) and their vasodilatory effect on small pial arteries and arterioles will regulate the cerebral blood flow. This effect is not included in Eqs. (38)–(40). Thus, these equations might underestimate the actual variation of smaller arterioles (i.e., vessels in the 3rd, 4th and 5th segments) during the early part of circulatory arrest. Preliminary studies [164] demonstrated that under the combination of the myogenic and chemical mechanisms, the changes of the arterial vessels have similar tendency as that of the case under the myogenic mechanism.

Solving Eqs. (33)–(36), one can obtain the hydraulic pressure at the inlet and outlet of the vascular segment, q_{ai} or q_{vi} . Therefore, the blood flow rate in each vascular compartment in the model of oxygen transport can be obtained as

$$\begin{aligned} Q_{ai} &= \frac{q_{a(i-1)} - q_{ai}}{R_{ai}}, & Q_{vi} &= \frac{q_{vi} - q_{v(i-1)}}{R_{vi}} \\ Q_c &= \frac{q_{am} - q_{vm}}{R_c} \quad (i = 1, 2, \dots, m) \end{aligned} \quad (41)$$

where, $q_{a0} = q_a$, $q_{v0} = q_v$. The changing blood flow $Q_{\text{deform } ai}$, $Q_{\text{deform } vi}$ due to capacitive effect are respectively expressed as

$$Q_{\text{deform } ai} = C_{ai} \frac{dq_{a(i-1)}}{dt}, \quad Q_{\text{deform } vi} = C_{vi} \frac{dq_{vi}}{dt} \quad (42)$$

The above mathematical models for the transient blood flow and oxygen transport in brain microcirculation allow a deeper understanding on the oxygen delivery during brain circulatory arrest. And some experimental results previously reported provide strong evidences to support them. Several conclusions from the simulation can be drawn such as [157]: (1) Variations in arteriolar vessels have only limited effect on

the transient blood flow and the oxygen transport. In contrast, the decreasing cerebral perfusion pressure is responsible for the hypoxia during the circulatory arrest; (2) Capacitive effect contributes little to the distribution of transient PO_2 ; (3) Venular PO_2 can be higher than the end-capillary PO_2 . This effect becomes more remarkable in the later time of circulatory arrest. At lower PO_2 , the PO_2 gradient in the first venular compartment can be larger than that of other postcapillary compartments and tissue. Extending the above model, one can have additional insight into the oxygen transport process with varied physiological and pathological conditions.

4.4.3 Temperature effects on the transport properties

Strictly speaking, parameters involved in the above models are generally space, time and temperature dependent. Particularly, temperature effect during brain cooling should be fully considered in order to analyze the brain cooling effect to the blood flow and oxygen transport. In such case, temperature becomes one of the most critical factors responsible for hemodynamics characteristics and oxygen consumption dynamics. In pure thermal opinion, lowering the temperature will lead to a decrease of the oxygen consumption rate, and an increase of blood viscosity, which will result in a more rapidly decreased blood flow rate. In the oxygen transport model, the temperature of cerebral tissue is of interest, which is however hard to define. To agree with the applied principle of lumped parameter in the compartmental model and to get an insight into the thermal influence on the oxygen transport during circulation arrest, Ji and Liu introduced an averaged ‘‘lumped brain temperature’’ $T_i(t)$ to characterize the overall temperature of the cerebral tissue, which reads as [157]

$$T_i(t) = \frac{\int_0^{R_0} T_h(r, t) \cdot 4\pi r^2 \cdot dr}{4\pi R_0^3 / 3} \quad (43)$$

where, $T_i(t)$ is the lumped brain temperature, which accounts for the temperatures over the whole cerebral tissue. Its effect on the oxygen transport and blood flow can then be easily incorporated into the compartmental model to test the development of brain hypothermia resuscitation.

Undoubtedly, oxygen metabolic rate M and oxygen diffusion coefficient E_i are closely associated with tissue temperature. Commonly, the oxygen consumption can be treated as following the first-order kinetics, i.e., $M = \beta C_i$ [91]. Taking into account the effect of temperature, the oxygen consumption rate is thereby expressed as [81]

$$M(C_i, T) = \beta C_i \cdot \eta^{[T(r,t) - 37]/10} \quad (44)$$

where $\beta = 4.7 \times 10^{-3} \text{ s}^{-1}$ is a constant, and η is temperature coefficient set as 2.5.

Studies [165,166] showed that the oxygen diffusion coefficient E_i increased with the temperature between 11°C and 37°C in an exponential manner that could be described

over the whole temperature range with a single temperature coefficient b determined by experimental data

$$E_i(T_t) = E_{i0} \cdot a \exp[b \cdot T_t] \quad (45)$$

where E_{i0} is the oxygen diffusion coefficient for each compartment at 37°C, $b = 4.6\%/^{\circ}\text{C}$ is the temperature coefficient for diffusion, and $a = 0.18$ is a constant.

Further, the effect of temperature on the blood flow behavior can also be dealt with. As is known, blood is a non-Newtonian fluid because its viscosity depends upon shear rate ($\dot{\gamma}$) [80]. Viscosity of blood asymptotically approaches its lowest level at shear rates higher than 150–200 s^{-1} (asymptotic viscosity). Under this range, blood can be considered as a Newtonian fluid with a constant viscosity. Since the Reynolds number characterizing the cerebral vascular flow is very small, it is assumed that the blood flow is a fully developed laminar pipe flow. Plasma viscosity approximates to the blood viscosity under this state. It depends on protein concentration, protein composition, hematocrit, as well as temperature. The variation in hematocrit measured for the same blood sample at different temperatures has been found to be less than 0.5% [80]. Temperature-dependent plasma viscosity of normal subjects, whose protein concentration is about 77.1 kg/m^3 , can be expressed as [157]

$$\mu_{\text{pl}} = 0.173 \times 10^{-3} \cdot \exp\left\{5.98 \times 10^7 / [T_i(t) + 273]^3\right\} \quad (46)$$

where μ_{pl} is the plasma viscosity.

Solving the above set of the basic compartmental governing equations will give out the blood flow and oxygen transport for the brain during hypothermia therapy.

It should be mentioned that, the vessel diameter d_i is dependent on the hydraulic blood pressure and temperature, but severe temperature reductions may impair vascular relaxation, called cold-induced “cerebrovasoparesis”. This effect is still difficult to quantify during hypothermia due to loss of vascular autoregulation. Besides, several points and limitations need to be mentioned for the above modeling: (1) The transient blood flow model is based on classifying the cerebral system into several segments similar to the model of oxygen transport, which is an approximate treatment of the actual situation since it might ignore the spatial variations of lumped parameters. Blood flow rate in each segment is assumed to be homogeneous. This approach may be only useful for the analysis of a whole organ. (2) In the above model, only the effect of the hemodynamic parameter, which is one of the most important factors responsible for the oxygen delivery deficit, was considered. However, other parameters contained in Eqs. (23)–(25), such as oxygen affinity, hematocrit, P_{50} , H^+ , S , and SCO , also change in a hypoxia process. But for simplicity, their effects on PO_2 were approximately omitted. (3) Some other limitations for the capillary bed include neglecting the intracapillary resistance to oxygen transport and assuming the constant capillary density under hypoxia. Besides, the role of tissue hypoxia in the auto-regulation of small cerebral arterioles, which needs

further research in the near future, was not included for simplicity.

4.5 Effect of circulation arrest on the cerebral oxygen level

At normal steady state, calculation on the distribution of output hydraulic pressure leaving each vascular compartment indicated that, the pressure decreases linearly from the inlet arterial pressure to the outlet venular pressure, which is close to zero. While in the arterial region, the pressure profile appears as having a much sharper gradient than that of the venular region. It is found that the pressure drop in the arterial network accounts for 83.3% of the total pressure drop between the inlet and the outlet of the vascular network, only 16.7% of the pressure drop occurs in postcapillary level [157]. The precapillary gradients of PO_2 are present over all arterioles. The PO_2 gradient increases in the successive branch of the arteriolar network and a significant PO_2 drop occurs in the capillaries. The PO_2 are approximately the same over the venular compartments [112]. It is noted that the PO_2 in the tissue compartment is lower than that of the postcapillary level, where the PO_2 in tissue is the lowest level in all compartments under the normal state.

For the transient oxygen pressure, calculation shows that the PO_2 gradient in the precapillary is enlarged with the reduced arteriolar PO_2 . The venular PO_2 gradually increases as blood flows from the first venular branch to the last one, which is consistent with the study of Pittman and Duling [165]. It is noted that the maximal PO_2 reduction occurs in the first venular compartment. In previous studies, Gutierrez [166] reported that the venous PO_2 can be higher than that of the end-capillary, and the difference becomes more remarkable during hypoxia. It can be predicted from the calculated data that PO_2 in the capillary, which is the most important source of oxygen supply, decreases to one half of that in the normal state, and PO_2 in the first venular branch becomes close to zero in about 10min. Clearly, since the PO_2 in the capillary reduces so rapidly, it will not be able to supply sufficient oxygen to tissue and will thus cause oxygen depletion in a short time.

When circulation arrest occurs, the regulatory change in the microcirculation includes variation of arteriolar diameters, which will result in an alteration of resistance and blood flow rate. In this case, myogenic reflex will be active and the arteriolar deformation is appreciably different from the passive case. As is calculated, the arteriolar pressure gradient decreases sharply with time. The outlet pressures leaving each arteriolar compartment are one order of magnitude smaller than their steady state value, i.e., a very small amount of blood flows through the vessels. The blood flowing through each vascular compartment also decreases sharply early on due to the rapidly decreasing hydraulic pressure. It is clear that the arteriolar pressure decreases so quickly that the reduced blood flow will no longer be able to supply sufficient oxygen, which undoubtedly results in a stagnant hypoxia in a short time. Further, it can be seen that variations in diameters

evidently increase the blood flow rate, especially during the first several minutes. Ye et al. have reported similar results [114–116] that the cerebral blood flow increases as arterial oxygen content falls with three different types of hypoxia. This is because the dilatory arterioles will reduce the cerebrovascular resistance, thus compensate for the reduced blood flow rate. The result reflects the regulatory response of microcirculation, which tends to maintain the blood flow constant and to some extent may alleviate the hypoxia at the onset of circulatory arrest.

4.6 Effects of cooling on the cerebral oxygen consumption dynamics

Few studies have been performed to analyze the hypothermia effect on the lower oxygen consumption dynamics during emergent rescue. Most of the existing studies were made to analyze the heat transport or oxygen transport independently. Only very limited research simultaneously addresses the coupled heat and oxygen transport behavior during brain cooling.

To examine the effect of different cooling on temperature development and oxygen consumption, Ji and Liu proposed a coupled heat-mass transfer model for characterizing the cerebral circulatory arrest using the classical Pennes bioheat equation and oxygen diffusion equation [80]. Two approaches, the surface cooling (water flowing around the brain surface) and the volumetric cooling (inserting a cooling probe into the deep brain or ventilating the cooling medium through the mouth and nose), have been tested. It can be found that the oxygen consumption rate differs little between the two surface convective cooling ($h_f = 10^\circ\text{C}$, $T_f = 20^\circ\text{C}$ and $h_f = 30^\circ\text{C}$, $T_f = 0^\circ\text{C}$), and the stored oxygen amount decreases sharply (Fig. 7). It is almost completely depleted within less than 20 minutes. At this time, the oxygen concentration is three orders of magnitude lower than the initial oxygen concentration. If the temperature of the brain cannot be quickly reduced, both the oxygen diffusion coefficient $D_i(T)$ and

the oxygen consumption rate $M(C_i, T)$ will remain at a higher value due to the weak cooling effect. Overall, the stored oxygen amount is depleted so quickly that it cannot meet the basic metabolic requirement, which may cause brain injury. Therefore, surface cooling is not very useful in reducing the oxygen consumption and thus preventing patients from brain injury.

In order to improve brain hypothermia resuscitation and prolong the patient's survival time, an alternative cooling approach, the volumetric cooling, should be used. Compared with the case of surface cooling, the oxygen concentration by volumetric cooling decreases much more slowly. When the uniform brain temperature changes from 15°C to 5°C through the volumetric cooling method, the average oxygen concentration decreases by 46% and 15% after about 20 min, respectively. The oxygen consumption rate at this case is several orders of magnitude lower than that at the case of surface cooling. Therefore, it is likely that the temperature decrease in the whole brain ensures the oxygen demand sufficient to permit tolerance for a long period of absent oxygen delivery.

However, there are also quite a few disputes arguing that the blood viscosity would increase with the decrease of temperature, which may lead to an increase of cerebral vascular resistance and thus worsen the hypoxia state. Reasons partially leading to this can be attributed to that, although extensive studies have been performed on the effect of hypothermia and circulatory arrest on cerebral blood flow and metabolism [1,43,54,80], few took into account the contribution of cerebral temperature changes to the hemodynamic parameters and thus the oxygen consumption in the case of circulatory arrest. Therefore, over the past few years, researchers kept arguing about the advantages and shortcomings of hypothermia on the brain resuscitation during circulation arrest. It is claimed that during circulation arrest, cooling the brain is also associated with some negative effects. For example, a high blood viscosity will be induced due to the reduction of temperature, which may lead to an increase in cerebral vascular resistance and thus reduced oxygen transport capability. In addition, the loss of pressure/flow autoregulation is most likely to occur due to the influence of deep hypothermic temperatures on vascular reactivity [91]. Further, the occurrence of shiver also enhances the oxygen consumption. Thus, a better understanding of the temperature effects on oxygen consumption dynamics is of importance in clinics. The compartmental model considering the temperature effects provides a very useful theoretical way to clarify such important issues [157]. Combined with the compartmental model including the temperature effect, the transient oxygen partial pressure (PO_2) distribution over the successive branches of the vascular network during circulation arrest was investigated by Ji and Liu [157]. Calculations indicated that the lower temperature is, the slower the decreasing rate for the PO_2 . Although immediately lowering the brain temperature may induce an evident increase in blood viscosity and subsequently a decrease in blood flow rate, which is responsible for oxygen transport, it always seems to result in

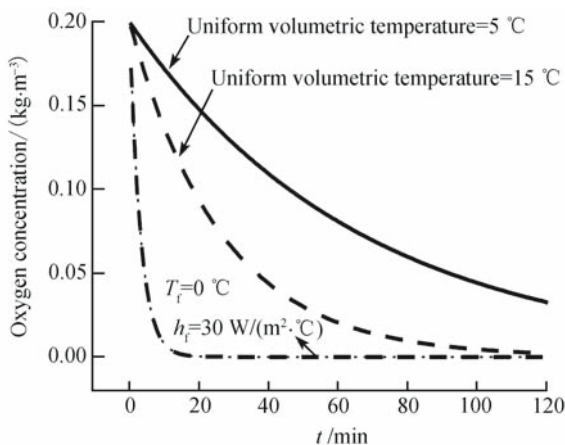


Fig. 7 The effect of two cooling approaches on oxygen concentration in the inner brain region ($r = 0.01$ m)

a monotonic increase of PO_2 . Therefore, applying a delayed hypothermia at the time when circulation completely stops cannot help a lot for the brain to sustain a longer period of oxygen depletion, compared with that of immediate cooling. These results strongly supported the idea that the lower the lumped brain temperature in the physiological range, the more beneficial the hypothermia effects on the patients, and cooling the brain should be performed as soon as possible once the circulation arrest occurs. The results indicated that hypothermia would always suppress the oxygen consumption and would monotonically increase the PO_2 in the successive branch of the vascular network. Thus from the current mathematical view point, lowering the temperature of the brain to protect its function during circulation arrest should be done as early as possible. The results accord well with the currently available experimental findings.

5 Ways for oxygen delivery

The currently available methods to supply oxygen for a patient with hypoxia are generally too slow to be effective. In emergency clinics, a patient with hypoxia is usually allowed to respire with supplemental oxygen. However, there exist a series of barriers before oxygen can be transported to the important organs. For example, this method may not be able to deliver oxygen to the anoxic tissue very timely. The life of the patient therefore is still subjected to loss. Other than the above effort, clinicians also try to deliver oxygen to tissues through vein injection. But when circulation arrest occurs, this method will not be valid. Clearly, if the oxygen level at the anoxic tissue can be improved even for minutes, the result would be quite different.

Overall, indirect oxygen delivery methods have been tried for many years. However, there is at present no ideal way to deliver oxygen directly to the target tissues inside the deep parts of the body. Gui and Liu proposed a promising approach [167], which is based on injecting a solution with high oxygen content into the tissues (Fig. 8). The cooling solution is administered to decrease the consumption rate of oxygen

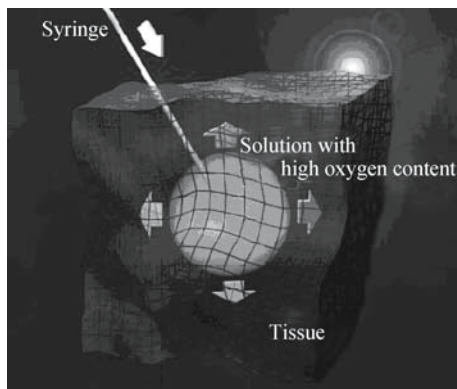


Fig. 8 Schematic for directly delivering oxygen to the target tissues in the deep biological body

and thus lengthen the endurable time for the patient. This is expected to spare more valuable time for a clinical rescue. Other than the above application, selectively supplying oxygen to the specific organs or tissues is also critical for some newly emerging bioengineering fields such as cell transplantation or tissue culture. To analyze the feasibility of the method, Gui and Liu built a mathematical model to characterize this multi-mode transport process, which is simultaneously coupled with fluid flow, heat transport and mass diffusion events [167]. Numerical calculation indicates that, this method has double significance for clinical practice. One is to help increase the local oxygen concentration of target tissue within a very short time. The other lies in that injection of the cooling solution also decreases the temperature of the tissues, which then significantly lowers the oxygen consumption rate. Both features will help to realize a much higher oxygen concentration and maintain the oxygen level in tissues during the hypoxia state. This method is expected to win a lot of valuable time for the patients to be sustained longer for emergency rescue.

6 Conclusion

As explained above, the currently available cooling methods can still not meet the requirement to quickly cool important organs such as the brain at the early part of circulatory arrest. Without any doubt, many clinical as well as engineering issues are urgently waiting for solutions. For each of the specific cooling strategies, tremendous theoretical modeling and experimental measurements should be conducted. The academic endeavors along this direction will not just produce a “useful” result for clinical practices, but may also open some new insights for better understanding the nature of the thermal mechanisms of the biological body, especially the cerebral tissues. Therefore, investigation into brain cooling appears not as an end but just as a start. It can be expected that more exciting fundamental discoveries will be certainly made in the near future.

Acknowledgements This work was supported by the National Natural Science Foundation of China (Grant No. 50325622).

References

1. Michenfelder M D, Mild J H. The relationship among canine brain temperature, metabolism, and function during hypothermia. *Anesthesiology*, 1991, 75: 130–136
2. Lv YG, Liu J. Effect of dendritic cell structure on enhancing oxygen transport in neuron. *Forschung in Ingenieurwesen-Engineering Research*, 2004, 68: 155–168
3. Tateishi N, Suzuki Y, Soutani M, et al. Flow dynamics of erythrocytes in microvessels of isolated rabbit mesentery: cell-free layer and flow resistance. *J Biomechanics*, 1994, 27: 1 119–1 125
4. Ursino M, Iezzi M, Stocchetti N. Intracranial pressure dynamics in patients with acute brain damage: a critical analysis with the aid of a mathematical model. *IEEE Trans Biomed Eng*, 1995, 42: 529–549

5. Ursino M. A mathematical model of overall cerebral blood flow regulation in the rat. *IEEE Trans Biomed Eng*, 1991, 38: 795–807
6. Czosnyka M, Richards H, Pichard J D, et al. Frequency-dependent properties of cerebral blood transport—an experimental study in anaesthetized rabbits. *Ultrasound in Med & Biol*, 1994, 20: 391–399
7. Greeley W J, Kern F H, Meliones J N, et al. Effect of deep hypothermia and circulatory arrest on cerebral blood flow and metabolism. *Ann Thorac Surg*, 1993, 56: 1 464–1 466
8. Steen PA, Newberg L, Milde J H, et al. Hypothermia and barbiturates: individual and combined effects on canine cerebral oxygen consumption. *Anesthesiology*, 1983, 58: 527–532
9. Popel A S, Pittman R N, Ellsworth M L. Rate of oxygen loss from arterioles is an order of magnitude higher than expected. *Am J Physiol*, 1989, 256: H921–H924
10. Bennett R A O, Pittman R N, Sullivan S M. Capillary spatial pattern and muscle fiber geometry in three hamster striated muscles. *Am J Physiol*, 1991, 260: H579–H585
11. Kiyatkin EA. Brain hyperthermia during physiological and pathological conditions: causes, mechanisms, and functional implications. *Current Neurovascular Research*, 2004, 1: 77–90
12. Mariak Z, Jadeszko M, Lewko J, et al. No specific brain protection against thermal stress in fever. *Acta Neurochir*, 1998, 140: 585–590
13. Wang H, Olivero W, Lanzino G, et al. Rapid and selective cerebral hypothermia achieved using a cooling helmet. *J Neurosurg*, 2004, 100: 272–277
14. Safar P. Resuscitation from clinical death: pathophysiologic limits and therapeutic potentials. *Crit Care Med*, 1988, 16: 923–941
15. Althaus N. Management of profound accidental hypothermia with cardiorespiratory arrest. *Ann Surg*, 1982, 195: 492–495
16. Sterz F, Safar P, Tisherman S, et al. Mild hypothermic cardiopulmonary resuscitation improves outcome after prolonged cardiac arrest in dogs. *Crit Care Med*, 1991, 19: 379–389
17. Ice Slurry Cooling to Induce Protective Heart and Brain Hypothermia. 2004-08-19, http://www.et.anl.gov/sections/tem/highlights/ice_slurry_cooling.html
18. Watanabe T, Orita H, Kobayashi M, et al. Brain tissue pH, oxygen tension, and carbon dioxide tension in profoundly hypothermic cardiopulmonary bypass: comparative study of circulatory arrest, nonpulsatile low-flow perfusion, and pulsatile low-flow perfusion. *J Thorac Cardiovasc Surg*, 1989, 97: 396–401
19. Leonov Y, Sterz F, Safar P, Radovsky A, Oku K, Tisherman S, Stezoski SW. Mild cerebral hypothermia during and after cardiac arrest improves neurologic outcome in dogs. *J Cereb Blood Flow Metab*, 1990, 10: 57–70
20. Zhu L., Diao C. Theoretical simulation of temperature distribution in the brain during mild hypothermia treatment for brain injury. *Medical and Biological Engineering and Computing*, 2001, 39: 681–687
21. D’Cruz B J, Fertig K C, Filiano A J, et al. Hypothermic reperfusion after cardiac arrest augments brain-derived neurotrophic factor activation. *Journal of Cerebral Blood Flow & Metabolism*, 2002, 22: 843–851
22. Dexter F. Mathematical analysis of haemodilution’s direct effect on rate of brain cooling during cardiopulmonary bypass. *Med Biol Eng Comput*, 1995, 33: 24–26
23. Dexter F, Hindman BJ. Computer simulation of brain cooling during cardiopulmonary bypass. *Ann Thorac Surg*, 1994, 57: 1 171–1 179
24. Corrad F. Selective brain cooling. *Arch Pediatrice*, 1999, 6: 87–92
25. Caputa M. Selective brain cooling: a multiple regulatory mechanism. *J Therm Biol*, 2004, 29: 691–702
26. Parmeggiani P L, Azzaroni A, Calasso M. A pontine-hypothalamic temperature difference correlated with cutaneous and respiratory heat loss. *Respiration Physiol*, 1998, 114: 49–56
27. Hayward J N, Baker M A. A comparative study of the role of the cerebral arterial blood in the regulation of brain temperature in five mammals. *Brain Res*, 1969, 16: 417–440
28. Azzaroni A, Parmeggiani P L. Changes in selective brain cooling across the behavioral states of the ultradian wake-sleep cycle. *Brain Res*, 1999, 844: 206–209
29. Baker M A. Brain cooling in endotherms in head and exercise. *Ann Rev Physiol*, 1982, 44: 85–96
30. Fuller A, Carter R N, Mitchell D. Brain and abdominal temperatures at fatigue in rats exercising in the heat. *J Appl Physiol*, 1998, 84: 877–883
31. Jessen C. Brain cooling: an economy mode of temperature regulation in artiodactyls. *News Physiol Sci*, 1998, 13: 281–286
32. Cabanac M. Selective brain cooling in humans: “fancy” or fact? *FASEB J*, 1993, 7: 1 143–1 147
33. Brengelmann G L. Specialized brain cooling in humans. *FASEB J*, 1993, 7: 1 148–1 153
34. Nielsen B. Natural cooling of the brain during outdoor bicycling? *Pflugers Arch*, 1988, 411: 456–461
35. Zhu L. Theoretical evaluation of contributions of heat conduction and countercurrent heat exchange in selective brain cooling in humans. *Ann Biomed Eng*, 2000, 28: 269–277
36. Maloney SK, Mitchell G. Selective brain cooling: role of angularis oculi vein and nasal thermoreception. *Am J Physiol*, 1997, 273: R1 108–R1 116
37. Johnsen H K, Blix B S, Mercer J B, et al. Selective cooling of the brain in reindeer. *Am J Physiol*, 1987, 253: R848–R853
38. Hindman B J, Dexter F. Estimating brain temperature during hypothermia. *Anesthesiology*, 1995, 82: 329–330
39. Ao H, Moon J K, Tanimoto H, et al. Jugular vein temperature reflects brain temperature during hypothermia. *Resuscitation*, 2000, 45: 111–118
40. Irmak M K, Korkmaz A, Eroglu O. Selective brain cooling seems to be a mechanism leading to human craniofacial diversity observed in different geographical regions. *Med Hypotheses*, 2004, 63: 974–979
41. Chochinov A H, Baydock B M S, Bristow G K, et al. Recovery of a 62-year-old man from prolonged cold water submersion. *Ann Emerg Med*, 1998, 31: 127–131
42. Trubel H, Herman P, Kampmann C, et al. Duration of induced seizures during selective pharyngeal brain cooling. *Biomed Tech*, 2004, 49: 279–281
43. Olsen R W, Hayes L J, Wissler E H, et al. Influence of hypothermia and circulatory arrest on cerebral temperature distributions. *ASME J Biomech Eng*, 1985, 107: 354–360
44. Ji Y, Liu J. Numerical simulation on cerebral thermal assembly during circulatory arrest. *Progress in Natural Science*, 2001, 11: 853–859 (in Chinese)
45. Laptook A R, Shalak L, Corbett R J T. Differences in brain temperature and cerebral blood flow during selective head versus whole-body cooling. *Pediatrics*, 2001, 108: 1 103–1 110
46. Ibayashi S, Takano K, Ooboshi H, et al. Effect of selective brain hypothermia on regional cerebral blood flow and tissue metabolism using brain thermo-regulator in spontaneously hypertensive rats. *Neurochem Res*, 2000, 25: 369–375
47. Wass C T, Waggoner J R, Cable D G, et al. Selective convective brain cooling during hypothermic cardiopulmonary bypass in dogs. *Ann Thorac Surg*, 1998, 66: 2 008–2 014
48. Smirnov OA. Method of increasing the efficiency of air hypotherms and an apparatus for cranio-cerebral cooling. *Biomed Eng*, 1969, 3: 257–260
49. Kolenko EA, Bezukh M S. Electronic device for hypothermia of the brain. *Biomed Eng*, 1971, 5: 239–241 (English translation of *Meditinskaya Tekhnika*)
50. Tooley J, Satas S, Eagle R, et al. Significant selective head cooling can be maintained long-term after global hypoxia ischemia in newborn piglets. *Pediatrics*, 2002, 109: 643–649

51. Bartoo C H. Cool cap may prevent brain damage after difficult birth. May 14, 2004, <http://www.mc.vanderbilt.edu/reporter/?ID=3289>
52. Hagioka S, Takeda Y, Takata K, et al. Nasopharyngeal cooling selectively and rapidly decreases brain temperature and attenuates neuronal damage, even if initiated at the onset of cardiopulmonary resuscitation in rats. *Crit Care Med*, 2003, 31: 2 502–2 508
53. Trubel H, Herman P, Kampmann C, et al. A novel approach for selective brain cooling: implications for hypercapnia and seizure activity. *Intens Care Med*, 2004, 30: 1 829–1 833
54. Mariak Z, White M D, Lewko J, et al. Direct cooling of the human brain by heat loss from the upper respiratory tract. *J Appl Physiol*, 1999, 87: 1 609–1 613
55. Harris S B, Darwin M G, Russell S R, et al. Rapid (0.5 degrees C/min) minimally invasive induction of hypothermia using cold perfluorochemical lung lavage in dogs. *Resuscitation*, 2001, 50: 189–204
56. Einer-Jensen N, Khoroshi M H. Cooling of the brain through oxygen flushing of the nasal cavities in intubated rats: an alternative model for treatment of brain injury. *Exp Brain Res*, 2000, 130: 244–247
57. Einer-Jensen N, Khoroshi M H, Petersen M B, et al. Rapid brain cooling in intubated pigs through nasal flushing with oxygen: prevention of brain hyperthermia. *Acta Vet Scand*, 2001, 42: 459–464
58. Desruelle A V, Candas V. Thermoregulatory effects of three different types of head cooling in humans during a mild hyperthermia. *Eur J Appl Physiol*, 2000, 81: 33–39
59. Saito J, Kurata Y, Takeyama Y, et al. Rapid development of brain hypothermia using femoral-carotid bypass. *Acad Emerg Med*, 2001, 8: 303–308
60. Luan X D, Li J, McAllister J P, et al. Regional brain cooling induced by vascular saline infusion into ischemic territory reduces brain inflammation in stroke. *Acta Neuropathol*, 2004, 107: 227–234
61. Hansebout R R, Peterson E W, Ringer T R, et al. Experience with core temperature maintenance during the course of regional profound brain hypothermia. *Med Res Eng*, 1970, 9: 9–13
62. Sumbatov L A. Local hypothermia in neurosurgery and its technical provision. *Biomed Eng*, 1974, 8: 271–273 (English translation of *Meditsinskaya Tekhnika*)
63. Li J, Luan X, Lai Q, et al. Long-term neuroprotection induced by regional brain cooling with saline infusion into ischemic territory in rats: a behavioral analysis. *Neurol Res*, 2004, 26: 677–683
64. Ding Y C, Li L, Luan X D, et al. Local saline infusion into ischemic territory induces regional brain cooling neuroprotection in rats with transient middle cerebral artery occlusion. *Neurosurgery*, 2004, 54: 956–964
65. Wen Y S, Huang M S, Lin M T, et al. Hypothermic retrograde jugular perfusion reduces brain damage in rats with heatstroke. *Crit Care Med*, 2003, 31: 2 641–2 645
66. Furuse M, Ohta T, Ikenaga T, et al. Effects of intravascular perfusion of cooled crystalloid solution on cold-induced brain injury using an extracorporeal cooling-filtration system. *Acta Neurochir*, 2003, 145: 983–993
67. Kuhnen G, Bauer R, Walter B. Controlled brain hypothermia by extracorporeal carotid blood cooling at normothermic trunk temperatures in pigs. *J Neurosci Meth*, 1999, 89: 167–174
68. Ji Y, Liu J. New conceptual method for directly cooling the target biological tissues. *Warme-und Stoffübertragung-Heat and Mass Transfer*, 2004, 41: 226–238
69. Wass C T, Waggoner J R, Cable D G, et al. Selective convective brain cooling during normothermic cardiopulmonary bypass in dogs. *J Thorac Cardiovasc Surg*, 1998, 115: 1 350–1 357
70. Kaukuntla H, Walker A, Harrington D, et al. Differential brain and body temperature during cardiopulmonary bypass—a randomised clinical study. *Eur J Cardio-Thorac*, 2004, 26: 571–578.
71. Fuller A, Mitchell G, Mitchell D. Non-thermal signals govern selective brain cooling in pigs. *J Comp Physiol B*, 1999, 169: 605–611
72. Trubel H, Herman P, Kampmann C, et al. Selective brain cooling from the pharynx. *Biomed Tech*, 2003, 48: 298–300
73. Iatrou C C, Domaingue C M, Thomas R D, et al. The effect of selective brain cooling on intracerebral temperature during craniotomy. *Anaesth Intens Care*, 2002, 30: 167–170
74. Boston U S, Sungurtekin H, McGregor C G A, et al. Differential perfusion: a new technique for isolated brain cooling during cardiopulmonary bypass. *Ann Thorac Surg*, 2000, 69: 1 346–1 350
75. Kaukuntla H, Harrington D, Bilkoo I, et al. Temperature monitoring during cardiopulmonary bypass—do we undercool or overheat the brain? *Eur J Cardio-Thorac*, 2004, 26: 580–584
76. Maloney S K, Fuller A, Mitchell G, et al. Rectal temperature measurement results in artifactual evidence of selective brain cooling. *Am J Physiol-Reg I*, 2001, 281: 108–114
77. Nagasaka T, Brinell H, Hales J R S, et al. Selective brain cooling in hyperthermia: the mechanisms and medical implications. *Med Hypothermia*, 1998, 50: 203–211
78. Nelson DA, Nunneley SA. Brain temperature and limits on transcranial cooling in humans: quantitative modeling results. *Eur J Appl Physiol Occup Physiol*, 1998, 78: 353–359
79. Trezek G. J, Jewett D L. Nodal network simulation of transient temperature fields from cooling sources in anesthetized brain. *IEEE Trans Bio-Med Eng*, 1970, BME-17: 281–286
80. Xu X J, Tikuisis P, Giesbrecht G. A mathematical model for human brain cooling during cold-water near-drowning. *J Appl Physiol*, 1999, 86: 265–272
81. Ji Y, Liu J. Preliminary study on the oxygen consumption dynamics during brain hypothermia resuscitation. In: *Proceedings of the 23rd Annual EMBS International Conference*. Istanbul, Turkey, 2001: 266–269
82. Mellergard P. Changes in human intracerebral temperature response to different methods of brain cooling. *Neurosurgery*, 1992, 31: 671–677
83. Diao C, Zhu L, Wang H. Cooling and rewarming for brain ischemia or injury: theoretical analysis. *Annals of Biomedical Engineering*, 2003, 31: 346–353.
84. Vietla S, Eberhart R C, Meyer D M. Influences of hypothermia and tissue perfusion on temperature distributions in simulated cranial surgery. *American Society of Mechanical Engineers, Heat Transfer Division, Advances in Bioheat and Mass Transfer*, 1993, 268: 9–17
85. Sukstanskii A L, Yablonskiy D A. An analytical model of temperature regulation in human head. *J Therm Biol*, 2004, 29: 583–587
86. Dennis B H, Eberhart R C, Dulikravich G S, et al. Finite-element simulation of cooling of realistic 3-D human head and neck. *ASME Journal of Biomechanical Engineering*, 2003, 125: 832–840
87. Xu LX, Liu J. Discussion of non-equilibrium heat transfer in biological systems. *Advances in Heat and Mass Transfer in Biotechnology*, 1998, 362: 13–17
88. Tien CL, Vafai K. Convective and radiative heat transfer in porous media. *Adv Appl Mech*, 1990, 27: 225–281
89. Lv Y G, Liu J. Capacity of brain cooling via ventilating oxygen at low temperature over respiratory tract. In: *Proceedings of 27th Annual International Conference of the IEEE Engineering in Medicine and Biology Society (IEEE-EMBS)*. Shanghai, China, 2005: 6 793–6 796
90. Hanna L M, Scherer P W. A theoretical model of localized heat and water vapor transport in the human respiratory tract. *ASME Journal of Biomechanical Engineering*, 1986, 108: 19–27
91. Popel A S. Theory of oxygen transport to tissue. *Critical Review in Biomedical Engineering*, 1989, 17: 257–321

92. Krogh A. The number and distribution of capillaries in muscles with calculations of the oxygen pressure head necessary for supplying the tissue. *J Physiol*, 1919, 52: 409–415
93. Knisely M H, Reneau D J D, Bruley D F. The development and use of equations for predicting the limits on the rates of oxygen supply to the cells of living tissues and organs: a contribution to the biophysics of health and disease. *Angiol J Vasc Dis*, 1969, 20: S1–S11
94. Grunewald W A, Sowa W. Capillary structures and O₂ supply to tissue: an analysis with a digital diffusion model as applied to the skeletal muscle. *Rev Physiol Biochem Pharmacol*, 1977, 77: 149–209
95. Popel A S. Analysis of capillary-tissue diffusion in multicapillary systems. *Math Biosci*, 1978, 39: 187–211
96. Metzger H. The influence of space-distributed parameters on the calculation of substrate and gas exchange in microvascular units. *Math Biosci*, 1976, 30: 31–35
97. Popel A S, Gross J F. Analysis of oxygen diffusion from arteriolar networks. *Am J Physiol*, 1979, 237: H681–H689
98. Ellsworth M L, Pittman R N. Arterioles supply oxygen to capillaries by diffusion as well as by convection. *Am J Physiol*, 1990, 258: H1240–H1243
99. Swain D P, Pittman R N. Oxygen exchange in the microcirculation of Hamster retractor muscle. *Am J Physiol*, 1989, 256: H247–H255
100. Honig C R, Gayeski T E J. Precapillary O₂ loss and arteriovenous O₂ diffusion shunt are below the limit of detection in myocardium. *Adv Exp Med Biol*, 1989, 247: 591–599
101. Sharan M, Popel A S. A mathematical model of countercurrent exchange of oxygen between paired arterioles and venules. *Math Biosci*, 1988, 91: 17–34
102. Piiper J, Meyer M, Scheid P. Dual role of diffusion tissue gas exchange: blood-tissue equilibration and diffusion shunt. *Respir Physiol*, 1984, 56: 131–141
103. Rose C P, Goresky C A, Bach G G., Bassingthwaite J B, Little S. An vivo comparison of non-gaseous metabolite and oxygen transport in the heart. *Adv Exp Med Biol*, 1988, 222: 45–54
104. van Beek J H, Duljst P, Westerhof N. Heat shunts in canine myocardium at the arteriolar level. *FASEB J*, 1989, 3: 405–412
105. Sejrsen P, Tonnesen K H. Shunting by diffusion of inert gas in skeletal muscle. *Acta Physiol Scand*, 1972, 86: 82–91
106. Goldman D, Popel A S. Computational modeling of oxygen transport from complex capillary networks: relation on the microcirculation physiome. In: Eke A, Delpy D T, eds. *Oxygen Transport to Tissue XXI*, New York: Plenum Press, 1999
107. Liu J. Analogy between heat and mass transfer leads to new oxygen transport equations in vascularized biological tissues. In: American Society of Mechanical Engineers, Heat Transfer Division. *Proceedings of the ASME Heat Transfer Division*. Anaheim, California, 2004, 375: 733–742
108. Ji Y, Liu J. Vasculature based model for characterizing oxygen transport in skin tissues. *Warme-und Stoffubertragung-Heat and Mass Transfer*, 2004, 40: 627–637
109. Ivanov K P, Kislyakov Y Y, Samoilov M Q. Microcirculation and transport of oxygen to neurons of the brain. *Microvasc Res*, 1979, 18: 434–441
110. Sharan M, Jones M J D, Koehler R C, et al. A compartmental model for oxygen transport in brain microcirculation. *Ann Biomed Eng*, 1989, 17: 13–38
111. Sharan M, Popel A S, Hudak M L, et al. An analysis of hypoxia in sheep brain using a mathematical model. *Ann Biomed Eng*, 1998, 26: 48–59
112. Sharan M, Jones M J D, Koehler R C, et al. A compartmental model for oxygen transport in brain microcirculation. *Ann Biomed Eng*, 1989, 17: 13–38
113. Roth A C, Wade K. The effect of transmural transport in the microcirculation: a two gas species model. *Microvasc Res*, 1986, 32: 64–83
114. Ye G F, Moore T W, Jaron D. Contributions of oxygen dissociation and convection to the behaviour of a compartmental oxygen transport model. *Microvasc Res*, 1993, 46: 1–18
115. Ye G F, Moore W T, Burek D G. A compartmental model for oxygen-carbon dioxide coupled transport in the microcirculation. *Ann Biomed Eng*, 1994, 22: 464–479
116. Ye G F, Park J W, Basude R. Incorporating O₂-Hb reaction kinetics and the Fåhræus effect into a microcirculatory O₂-CO₂ transport model. *IEEE Trans Biomed Eng*, 1998, 45: 26–35
117. Ye G F, Jov D, Buerk D G., et al. O₂-Hb reaction kinetics and the Fåhræus effect during stagnant, hypoxic, and anemic supply deficit. *Ann Biomed Eng*, 1998, 26: 60–75
118. Lau Y Y, Abe T, Ewing A G, Voltammetric measurement of oxygen in single neurons using platinumized carbon ring electrodes. *Analytical Chemistry*, 1992, 64: 1 702–1 706
119. Busciglio J, Yankner B A. Apoptosis and increased generation of reactive oxygen species in Down's syndrome neurons in vitro. *Nature*, 1995, 378: 776–779
120. Fairchild M D, Parsons J E, Wasterlain C G, et al. A hypoxic injury potential in the hippocampal slices. *Brain Research*, 1988, 453: 357–361
121. Gage A T, Stanton P K. Hypoxia triggers neuroprotective alterations in hippocampal gene expression via a heme-containing sensor. *Brain Research*, 1996, 719: 172–182
122. He L Y, Chen W, Fan J P, et al. Model SH-SY5Y cells apoptosis induced by hypoxia/hypoglycemia. *China Journal of Basic Medicine in Traditional Chinese Medicine*, 2000, 6: 39–42 (in Chinese)
123. Pez Pinz M A, Mumford P L, Rosenthal M. Anoxia preconditioning in hippocampal slices: role of adenosine. *Neuroscience*, 1996, 75: 687–694
124. Khaspekov L, Shamloo M, Victorov I. Sublethal in vitro glucose-oxygen deprivation protects cultured hippocampal neurons against a subsequent severe insult. *Neuro Report*, 1998, 9: 1 273–1 276
125. Centeno J M, Orti M, Salom J B. Nitric oxide is involved in anoxic preconditioning neuroprotection in rat hippocampal slices. *Brain Research*, 1999, 836: 62–69
126. Ellsworth M L, Ellis C G, Popel A S, et al. Role of microvessels in oxygen supply to tissue. *NIPS*, 1994, 9: 119–123
127. Deng Z S, Liu J. Analytical study on bioheat transfer problems with spatial or transient heating on skin surface or inside biological bodies. *ASME J Biomech Eng*, 2002, 124: 638–649
128. Zhu L, Weinbaum S. Model for heat transfer from embedded blood vessels in two-dimensional tissue preparations. *ASME J Biomech Eng*, 1995, 117: 64–73
129. Durkee J W, Antich P P, Lee C E. Exact-solutions to the multiregion time-dependent bioheat equation. 1. solution development. *Phys in Med and Biol*, 1990, 35: 847–867
130. Durkee J W, Antich P P. Characterization of bioheat transport using exact solution to the cylindrical geometry, multiregion, time-dependent bioheat equation. *Phys in Med and Biol*, 1991, 36: 1 377–1 406
131. Liu J, Zhou Y X, Deng Z S. Sinusoidal heating method to noninvasively measure tissue perfusion. *IEEE Trans on Biomed Eng*, 2002, 49: 867–877
132. Chen M M, Holmes K R. Microvascular contributions in tissue heat transfer. *Ann New York Acad Sci*, 1980, 335: 137–150
133. Wulff W. The energy conservation equation for living tissues. *IEEE Trans Biomed Eng*, 1974, BME-21: 494–497
134. Charny C K. Mathematical models of bioheat transfer. *Adv Heat Transfer*, 1992, 22: 19–155
135. Huang H W, Chan C L, Roemer R B. Analytical solutions of Pennes bio-heat transfer equation with a blood vessel. *ASME J Biomech Eng*, 1994, 116: 208–212
136. Charny C K, Weinbaum S, Levin R L. Evaluation of the Weinbaum-Jiji bioheat equation for normal and hyperthermic conditions. *ASME J Biomech Eng*, 1990, 112: 80–87

137. Weinbaum S, Jiji L M, Lemons D E. Theory and experiment for the effect of vascular microstructure on surface tissue heat transfer-part I: anatomical foundation and model conceptualization. *ASME J Biomech Eng*, 1984, 106: 321–329
138. Jiji L M, Weinbaum S, Lemons D E. Theory and experiment for the effect of vascular microstructure on surface tissue heat transfer-part II: model formulation and solution. *ASME J Biomech Eng*, 1984, 106: 331–341
139. Weinbaum S, Jiji L M. A new simplified bioheat equation for the effect of blood flow on local average tissue temperature. *ASME J Biomech Eng*, 1985, 107: 131–137
140. Dagan Z, Weinbaum S, Jiji L M. Parametric studies on the three-layer microcirculatory model for surface tissue energy exchange. *ASME J Biomech Eng*, 1986, 108: 89–96
141. Ellsworth M L, Pittman R N. Heterogeneity of oxygen diffusion through hamster striated muscles. *Am J Physiol*, 1984, 246: H161–H167
142. Mahler M. Diffusion in an elliptical cylinder: a reassessment of the diffusion coefficient for oxygen in muscle. *Biophys J*, 1981, 33: 25–31
143. Kawashiro T, Nusse W, Scheid P. Determination of diffusivity of oxygen and carbon dioxide in respiring tissue: results in rat skeletal muscle. *Pfluegers Arch*, 1975, 359: 231–251
144. O'Brien J J, Lucey E C, Snider G L. Arterial blood gases in normal hamsters at rest and during exercise. *Respirat Environ Exercise Physiol*, 1979, 46: 806–810
145. Wittenberg J B. Myoglobin-facilitated oxygen diffusion: role of myoglobin in oxygen entry into muscle. *Physiol Rev*, 1970, 50: 559–636
146. Whitmore R L. *Rheology of Circulation*. London: Pergamon Press, 1968, 23–45
147. Salathe E P. Mathematical modeling of oxygen transport in skeletal muscle. *Math Biosci*, 1982, 58: 171–184
148. Harris P D. Movement of oxygen in skeletal muscle. *News Physiol Sci*, 1986, 1: 147–149
149. Honig C R, Gayeski T E J. Arteriovenous oxygen diffusion shunt is negligible in resting and working gracilis muscles. *Am J Physiol*, 1991, 261: H2 031–H2 043
150. Kuo L, Pittman R N. Effect of hemodilution on oxygen transport in arteriolar networks of hamster striated muscle. *Am J Physiol*, 1988, 254: H331–H339
151. Sarelius I H, Duling R R. Microvascular adaptations during maturation of striated muscle. *Am J Physiol*, 1981, 241: H317–H324.
152. Moore J A, Ethier C R. Oxygen mass transfer calculations in large arteries. *ASME J Biomech Eng*, 1997, 119: 469–475
153. Hsu R, Secomb T W. Analysis of oxygen exchange between arterioles and surrounding capillary-perfused tissue. *ASME J Biomech Eng*, 1992, 114: 227–231
154. Weerappuli D P V, Popel A S. A model of oxygen exchange between an arteriole or venule and the surrounding tissue. *ASME J Biomech Eng*, 1989, 111: 24–31
155. Secomb T W, Hsu R. Simulation of O₂ transport in skeletal muscle: diffusive exchange between arterioles and capillaries. *Am J Physiol*, 1994, 267: H1 214–H1 221
156. Li Z, Yipintsoi T, Bassingthwaite JB. Nonlinear model for capillary-tissue oxygen transport and metabolism. *Ann Biomed Eng*, 1997, 25: 604–619
157. Ji Y, Liu J. Numerical study on the effect of lowering temperature on the oxygen transport during brain hypothermia resuscitation. *Computers in Biology and Medicine*, 2002, 32: 495–514
158. Samaja M, Gattinoni L. Oxygen affinity in the blood of sheep. *Respir Physiol*, 1978, 34: 385–392
159. Winslow R W, Swenberg M L, Berger R L, et al. Oxygen equilibrium curve of normal blood and its evaluation by Adair equation. *J Bio Chem*, 1977, 252: 2 331–2 337
160. Ursino M, Giammarco P D, Belardinelli E. A mathematical model of cerebral blood flow chemical regulation-part 1: diffusion processes. *IEEE Trans Biomed Eng*, 1989, 36: 183–191
161. Ursino M, Giammarco P D, Belardinelli E. A mathematical model of cerebral blood flow chemical regulation-part 2: reactivity of cerebral vascular bed. *IEEE Trans Biomed Eng*, 1989, 36: 192–201
162. Ursino M, Magosso E. Role of tissue hypoxia in cerebrovascular regulation: a mathematical modeling study. *Ann Biomed Eng*, 2001, 29: 563–574
163. Cavalcanti S, Ursino M. Chaotic oscillations in microvessel arterial networks. *Ann Biomed Eng*, 1996, 24: 37–47
164. Ursino M, Fabbri G. Role of the myogenic mechanism in the genesis of microvascular oscillations (vasomotion): analysis with a mathematical model. *Microvasc Res*, 1992, 43: 156–177
165. Pittman R N, Duling B R. The determination of oxygen availability in the microcirculation. In: Jobsis F F, ed. *Oxygen and Physiological Function*. Dallas: Professional Information Library, 1977, 133–147
166. Gutierrez G. The rate of release and its effect on capillary O₂ tension: a mathematical analysis. *Respir Physiol*, 1986, 63: 79–96
167. Gui L, Liu J. Simulation of delivering oxygen directly to the target tissues by injection. *Int J Thermal Sci*, 2006, 45: 528–535